MATHEMATICAL MODELING OF COVID-19 TRANSMISSION AND VACCINATION: THE CASE OF UAE

by

Manal W. Almuzini

A thesis presented to the Faculty of the

American University of Sharjah

College of Arts and Sciences

in Partial Fulfillment

of the Requirements

for the Degree of

Master of Science in

Mathematics

Sharjah, UAE

June 2022

Declaration of Authorship

I declare that this thesis is my own work and, to the best of my knowledge and belief, it does not contain material published or written by a third party, except where permission has been obtained and/or appropriately cited through full and accurate referencing.

Signature ……Manal W. Almuzini……

Date……..…….……23/06/2022……

Approval Signatures

We, the undersigned, approve the Master's Thesis of Manal Walid Kamel Almuzini

Title: MATHEMATICAL MODELING OF COVID-19 TRANSMISSION AND VACCINATION: THE CASE OF UAE

Date of Defense: 23-06-2022

Name, Title, and Affiliation	**Signature**
Dr. Abdul Salam Jarrah Professor, Department of Mathematics & Statistics, Thesis Co-advisor	
Dr. Hana Sulieman Professor, Department of Mathematics & Statistics, Thesis Co-advisor	
Dr. Ziyad Sharawi Associate Professor, Department of Mathematics & Statistics, Thesis Committee Member	
Dr. Sarah Dalibalta Associate Professor, Department of Biology, Chemistry & Envir. Sciences Thesis Committee Member	
Dr. Abdul Salam Jarrah Department Head and Program Coordinator Department of Mathematics & Statistics, American University of Sharjah	
Dr. Hana Sulieman Associate Dean for Graduate Studies College of Arts and Sciences	
Dr. Mahmoud Anabtawi Dean College of Arts and Sciences	
Dr. Mohamed El-Tarhuni Vice Provost for Research & Graduate Studies Office of Research & Graduate Studies	

Acknowledgments

This project would not have been completed without the support of many people. Many thanks to my advisors, Dr. Abdul Salam Jarrah and Dr. Hana Sulieman, who were patient enough to read and review my numerous revisions. Thanks to my external examiners, Dr. Sarah Dalibalta and Dr. Ziyad Sharawi, for their insightful and valuable feedback that helped further enhance my thesis. I thank the American University of Sharjah; I am proud to be a graduate of AUS. Many thanks to my family, husband, and children for their patience and encouragement. Finally, thanks to my friends, especially Ms. Safiyah Babiker, who always was there to support and help in Matlab coding.

Abstract

Mathematical models are widely used in simulating infectious diseases. They are employed to investigate the disease transmission dynamics, forecast its spreading pattern, check the effectiveness of the interventions, or any other point of interest regarding the disease progression. In general, models are expressed in terms of Differential Equations. In this thesis, we propose a mathematical model called the SEIR-VD model (S: Susceptible, E: Exposed, I: Infected, R: Recovered, V: Vaccinated, and D: Deaths) to study the COVID-19 progression and forecast its spreading. We examine the model characteristics and complete its mathematical analysis (stability points, basic reproduction number, and sensitivity analysis). We use the data of the UAE during the vaccination intervention as a case study. Our numerical analysis includes parameter estimation, curve fitting, prediction, and model validation. For the numerical analysis of our proposed SEIR-VD model, we employed a switched hybrid forced model developed in [1] for which the main time interval is divided into sub-intervals, and over these sub-intervals, the model parameters are forced to be a time-dependent function with the time considered continuous for some selected parameters and discrete for others. Different scenarios for vaccine intervention are considered in order to determine certain rates of fully immunized population. The proposed model can be used to investigate COVID-19 dynamics in other countries when relevant data are available to feed the model.

Keywords: *COVID-19, Ordinary differential equation models, Susceptible Infected Recovered-SIR, Susceptible Exposed Infected Recovered-SEIR*

Table of Contents

Abstract **5**

List of Figures **8**

List of Tables **10**

Chapter 1 Introduction **11**

1.1 Background 11

1.2 Thesis Objectives 13

1.3 Thesis Structure 13

Chapter 2 Mathematical Modeling of COVID-19 **14**

2.1 Mathematical Modeling of Infectious Diseases 14

2.2 Review of Compartmental Models Applied To COVID-19 16

Chapter 3 SEIR-VD Epidemiological Model for COVID-19 **24**

3.1 SEIR-VD Mathematical Model Assumptions 24

3.2 SEIR-VD Mathematical Model Representation 25

3.3 Mathematical Analysis of the COVID-19 SEIR-VD Model 27

3.3.1 An invariant region 27

3.3.2 Disease free equilibrium point (DFEP) 29

3.3.3 Endemic equilibrium point (EEP) 30

3.3.4 The basic reproduction number is calculated using the next generation matrix (NGM) method 31

3.3.5 The basic reproduction number of our model and its role in disease free equilibrium point stability 34

3.3.6 Local sensitivity analysis of the basic reproduction number ($\Re_0$) 38

Chapter 4 The UAE Case Study: Numerical Analysis and Curve Fitting **43**

4.1 Introduction 43

4.2 Tools, Model Assumptions, and Calibrations 44

4.3 Parameter Estimation and Model Calibration Over the Whole Interval . 45

4.3.1 The graphical results of the curve fitting over the whole interval 46

4.4 General Workflow and Proposed Algorithm for the Proposed SEIR-VD Model 47

4.5 Switched Hybrid Dynamical System Approach 48

4.6 Bayesian Information Criterion (BIC) Approach 49
4.7 Infection Transmission Rate-β as a Forcing Continuous Function of Time 53
4.7.1 Basic reproduction number as a time-dependent function 55
4.7.2 Model validation 59
4.8 Results and Discussion 60
4.8.1 Original recorded data from [38]: 60
4.8.2 The switched hybrid forced model results 62
4.8.3 Prediction results using the last parameters estimated in Δ_4: . . 64
4.8.4 Vaccination intervention and prediction: 66
Chapter 5 Conclusion, Limitations, Discussions, and Future Work 68
References 70
Appendix A 75
Appendix B 76
Vita 79

List of Figures

Figure 2-1: Scheme of the classical model SIR. 14
Figure 2-2: Scheme of the classical model SEIR. 15
Figure 2-3: Scheme of the model SEIR studied in [18]. 17
Figure 2-4: Scheme of the model SEIR studied in [14]. 17
Figure 2-5: Scheme of the model SEIR studied in [19]. 18
Figure 2-6: Scheme of the extended SEIR model studied in [20]. 20
Figure 2-7: Scheme of the extended SEIR model studied in [1]. 21
Figure 2-8: Scheme of the extended SEIR model studied in [15] 22

Figure 3-1: Proposed extended SEIR-VD model. 25

Figure 4-1: Fitted curves of reported and predicted daily numbers of infected individuals from the third of July to 31 of August 2021 (60 days) in UAE. 46
Figure 4-2: Fitted curves of reported and predicted daily numbers of recovered individuals from the third of July to 31 of August 2021 (60 days) in UAE. 46
Figure 4-3: Fitted curves of reported and predicted daily numbers of deaths from the third of July to 31 of August 2021 (60 days) in UAE. 47
Figure 4-4: General workflow of the proposed algorithm for the SEIR-VD model 48
Figure 4-5: The sum value of the $BIC_n(Y)$ total for the infected, recovered, vaccinated, and deaths 51
Figure 4-6: Scheme of changing parameter values over the four sub-intervals of interest 54
Figure 4-7: The forced continuous function $\beta(t)$. 55
Figure 4-8: Basic reproduction number value over time. 56
Figure 4-9: The effect of vaccine's inefficiency $\sigma = 0.05$ on $\Re_0(t)$. 57
Figure 4-10: The effect of vaccine's inefficiency $\sigma = 0.1$ on $\Re_0(t)$. 57
Figure 4-11: The effect of vaccine's inefficiency $\sigma = 0.2$ on $\Re_0(t)$. 58
Figure 4-12: The effect of vaccine's inefficiency $\sigma = 0.3$ on $\Re_0(t)$. 58
Figure 4-13: Reported daily numbers of infected individuals from the third of July to mid September 2021 in UAE as in [38]. 60

Figure 4-14: Reported daily numbers of recovered individuals from the third of July to mid September 2021 in UAE as in [38]. 61
Figure 4-15: Reported daily numbers of deaths from the third of July to mid September 2021 in UAE as in [38]. 61
Figure 4-16: Reported daily total numbers of vaccinated individuals from the third of July to mid September 2021 in UAE as in [38]. 62
Figure 4-17: Fitted curves of infected individuals (reported and predicted from the third of July to 31 of August 2021 in UAE) [38]. 62
Figure 4-18: Fitted curves of recovered individuals (reported and predicted from the third of July to 31 of August 2021 in UAE) [38]. 63
Figure 4-19: Fitted curves of deaths (reported and predicted from the third of July to 31 of August 2021 in UAE) [38]. 63
Figure 4-20: The forecasting for 14 days starting from the first of September 2021 to 14-September 2021 of infected individuals. 64
Figure 4-21: The forecasting for 14 days starting from the first of September 2021 to 14-September 2021 of recovered individuals. 65
Figure 4-22: The forecasting for 14 days starting from the first of September 2021 to 14-September 2021 deaths. 65
Figure 4-23: Effects of κ increment on the total number of fully vaccinated individuals. 66

List of Tables

Table 3.1: List of variables and their definitions used in the proposed model. 26

Table 3.2: Parameters and their definitions in System (3.1). 27

Table 4.1: Estimated parameter values of γ, β, α, and ϵ for the four sub-intervals. 53

Table 4.2: Vaccine's inefficiency (σ) contribution to the basic reproduction number $\Re_0(t)$. 59

Table 4.3: Relative residuals of the infected (I), recovered (R), and deaths (D) for the period starting from the third of July to 31 of August 2021 in UAE. 64

Table 4.4: Relative residuals of the infected (I), recovered (R), and deaths (D) for the period starting from the first of September to mid September 2021 in UAE. 65

Table 4.5: Required vaccinated individuals per day to reach 80% and 85%. 67

Chapter 1: Introduction

1.1 Background

Epidemiological mathematical models are typically defined as mathematical representations of disease transmission epidemiology and its underlying mechanisms. They are vital tools in studying infectious disease progression and controlling its spreading. Epidemiological mathematical models were used from past times and were initially employed by the Swiss mathematician Daniel Bernoulli in 1760 [2] when he argued for inoculation to control and eradicate the smallpox disease in France.

Mathematical models have been used to study the infectious and non-infectious disease characteristics and to predict its future dynamics and behavior, such as breast cancer [3] as an example of a non-infectious disease, Ebola [4], and Malaria [5] as examples of infectious diseases. For infectious diseases, mathematical models showed perfect results in simulating the progression of the diseases and controlling their spread.

Severe acute respiratory syndrome corona virus-2 (SARS-CoV-2), which is known as COVID-19, is an infectious disease that is extremely transmissible. It was identified by the World Health Organization (WHO) as a global pandemic in March 2020 [6]. COVID-19 triggers the disease and has become particularly contagious, culminating in more than 8 million cases globally by June 2020 [6]. Human lives and lifestyles were seriously dominated and reshaped by the disease. Non-pharmaceutical interventions (NPIs) have been introduced by countries to limit the outbreak during its early stages. The predominant method to control the epidemic was stringent, including different types of lock-down and social restrictions, while appropriate treatment and vaccination interventions were yet to be explored and identified. As countries hit the height of the outbreak and the lack of treatments and vaccines, new guidelines were designed under various conditions of coexistence to reduce the economic impacts of complete or partial closing of businesses, colleges, stores, etc. These useful guidelines and precautions were mostly provided to politicians and decision-makers through researchers' feedback and recommendations, commonly built on scientific bases and experiences such as epidemiological mathematical models [7].

Many questions are faced by public health specialists and higher authorities during infectious disease spreading, especially during its early stages. For instance, what would be the severity of the epidemic? This question could be perceived in a number

of different ways. How many people, for example, would be impacted and would require medical attention? What would be the highest number of individuals who would require treatment at any given time? For how long would the outbreak last? How effective would quarantine be for people who were in contact with infected individuals? And how long would the quarantine decrease the spreading of the pandemic? Would the new vaccinations be effective in combating the pandemic? Would the vaccination process within a short time affect the infection curve positively or negatively based on the effectiveness of the vaccines? Would it be wise to make COVID-19 vaccinations available to all society's members on an equitable basis, in spite of the financial and political obstacles? What were the chances of eradicating or eliminating the disease under specific vaccination procedures? In general, models are employed in proposing, creating, comparing, evaluating, and developing different diagnoses, preventive, therapeutic, and control procedures [8, 9]. Finding answers to any of these questions would need a wide variety of classifications and properties of the mathematical models, which make each model specific with its own properties and structures.

Mathematical models can be categorized into classes based on the methodologies, aspects, structures, or designs on which they are built and used. For instance, if we consider the time factor, they will be classified into continuous or discrete mathematical models. While considering the space factor, then they will be either spatial (partial differential equations-PDEs) or non spatial (ordinary differential equations-ODEs). Others are classified as deterministic or stochastic, capturing the occurrence probability of the event to be changed from one state to another (e.g., change the person from the infected state into the recovered state or deaths state) [10].

Some researchers classify the epidemiological mathematical model into two broad categories data-driven models and mechanistic models [7]. Data-driven models depend on machine learning and statistical methods such as auto-regressive time series and deep learning for parameter estimation and forecasting [11]. The mechanistic models employ algorithmic and procedural methods to capture the dynamics of the infectious disease between individuals in the population. Recently, the combination of "data-driven models" and "mechanistic models" is spreading and is known as "hybrid models" [12, 13].

Mathematical models have been developed and used to simulate COVID-19 dynamics, control its spreading, and examine all possible interventions [14, 15, 13].

1.2 Thesis Objectives

The goals of this thesis are as follows:

- To develop a mathematical model to study the dynamic of the infectious disease COVID-19 and the effect of vaccine intervention.
- To study the proposed model's characteristics and dynamics, including sensitivity analysis and the basic reproduction number.
- To estimate the model's parameters, calibrate the model, and achieve a prediction stage using the data of UAE as a case study.
- To validate the model through graphical stages and numerical stages.

1.3 Thesis Structure

The remainder of this thesis is organized as follows: Chapter 2 provides an overview of some mathematical epidemiological models. Chapter 3 introduces the proposed Susceptible, Exposed, Infected, Recovered, Vaccinated, and Deaths-SEIRVD model mathematical study and its properties, sensitivity analysis, and computes its basic reproduction number. Chapter 4 presents some computational analysis (curve fitting, calibration, simulation, and parameter estimation) for the UAE as a case study in addition to the results, prediction, and model validation. Chapter 5 includes limitations, discussions, and future work.

Chapter 2: Mathematical Modeling of COVID-19

2.1 Mathematical Modeling of Infectious Diseases

Mathematical mechanistic models are widely used to represent the dynamics of infectious diseases, including COVID-19, and investigate the effects of interventions and treatments. In 1927, Kermack and McKendrick were the first to introduce the basic SIR (S: Susceptible, I: Infected, and R: Recovered) compartmental model formulation [16]. The diagram of the SIR model can be shown in Figure 2-1 as follows:

Figure 2-1: Scheme of the classical model SIR.

With the following system of nonlinear ordinary differential equations:

$$\begin{aligned} \frac{dS}{dt} &= -\beta S(t) * I(t), \\ \frac{dI}{dt} &= \beta S(t) * I(t) - \alpha I(t), \\ \frac{dR}{dt} &= \alpha I(t). \end{aligned} \tag{2.1}$$

This simple compartmental SIR model is formulated mathematically as a system of three ordinary differential equations (ODEs) as shown in System (2-1). Each equation reflects the rate of change of each compartment over time. This system has two parameters:

1. The infection transmission rate (β) influences the movement from the susceptible compartment to the infected compartment due to contact with an infected person.

2. The recovery rate (α) influences the movement from the infected compartment to the recovered compartment. It is determined by the inverse of the average of the recovery period of the disease measured in days.

One of the critical assumptions for the classical Susceptible-Infected-Recovered (SIR) model is considering homogeneous population mixing, which indicates that all individuals in the population have an equal chance of coming into contact with others. Another assumption is that the SIR model doesn't include demography, where it assumes that the population is closed with no births, deaths, or migration. Permanent immunity is gained, and individuals are turned to recovery after infection.

Many modifications and extensions have been developed to improve the quality of the ”classical SIR” model and to investigate the different complicated types of infectious diseases. Depending on the disease, these changes could be in the direction of the transmissions between the different compartments or adding more compartments in order to capture the various states of the individuals during the epidemic. One extension of the SIR model is the SEIR model, where “E” stands for the exposed compartment for those individuals who are infected but still not infectious. This is due to the latent or incubation period, as this incubation period is required for exposed individuals to develop symptoms. Adding the exposed state as an additional compartment to the SIR model to get the classical SEIR (S: Susceptible, E: Exposed, I: Infected, and R: Recovered) model is critical in simulating infectious disease with a latent period to be considered such as Ebola infectious disease [17]. The diagram of the classical SEIR model can be shown in Figure 2-2 as follows:

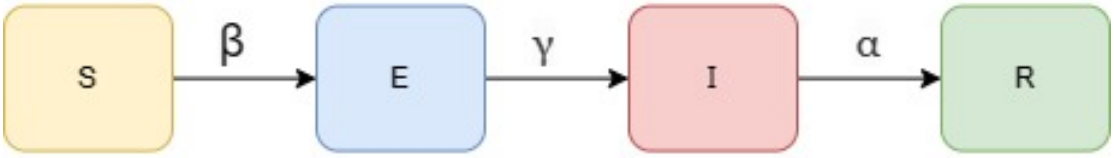

Figure 2-2: Scheme of the classical model SEIR.

With the following system of nonlinear ordinary differential equations:

$$\begin{aligned} \tfrac{dS}{dt} &= -\beta S(t) * I(t), \\ \tfrac{dE}{dt} &= \beta S(t) * I(t) - \gamma E(t), \\ \tfrac{dI}{dt} &= \gamma E(t) - \alpha I(t), \\ \tfrac{dR}{dt} &= \alpha I(t). \end{aligned} \tag{2.2}$$

This system has three parameters:

1. The infection transmission rate (β) influences the movement from the susceptible compartment to the exposed compartment due to contact with an infected person.

2. The transmission rate (γ) influences the movement from the exposed compartment to the infected compartment. It is determined by the inverse of the average of the incubation period of the disease measured in days.

3. The recovery rate (α), as defined in the System (2.1) of the SIR model.

Furthermore, additional compartments can be added to the classical SEIR model, such as quarantine (Q), deaths (D), or vaccinated (V) as various extensions to the SEIR model, depending on the purpose of the model. These additional compartments exist in order to account for the new requirements reflecting an increment in the number of differential equations in the system representing the model, where each compartment (state) is mathematically represented via a differential equation. Such changes and additions are playing vital roles in simulating the infectious disease phenomena under different hypotheses, answering the specific inquiries via achieving improvements in quantitative analysis.

The SIR and SEIR models, along with their various extensions, are used in recent literature on COVID-19 disease simulation and modeling. In the next section, we review some of these models and discuss some of their features along with their ODEs model formulation reflecting different aspects of the disease.

2.2 Review of Compartmental Models Applied To COVID-19

Compartmental models for simulating COVID-19 disease have recently been developed to examine its progress, control its spreading, and investigate possible interventions.

COVID-19 infected individuals are not considered to be contagious for a specific period due to the biological characteristics of the SARS-CoV-2. It is essential for COVID-19 modeling to incorporate the latent period via the exposed compartment (E:exposed) and the transmission rate γ as indicated and explained in System (2.2).

Several enhancements to the SEIR model were made in order to capture COVID-19 dynamics and examine its transmission. These enhancements can be implemented via the direction of the transmission between the different compartments. This will contribute to additional terms in the ODEs without affecting the total number of the differential equations. An example of such improvement in the SEIR model is shown in the following diagram as shown in Figure 2-3, where the authors added a backward arrow indicating the movement from the recovered state back to the susceptible state due to the loss of immunity:

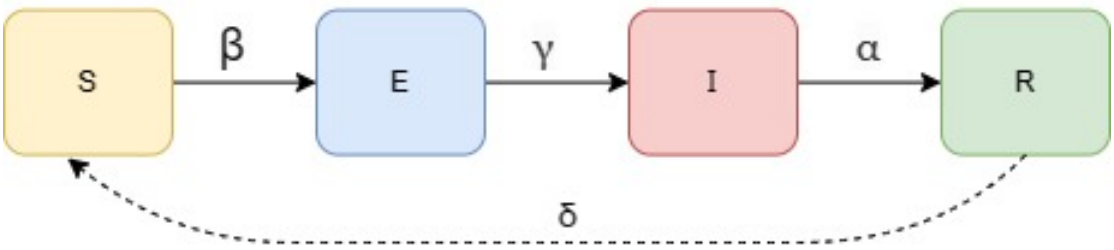

Figure 2-3: Scheme of the model SEIR studied in [18].

With the following system of nonlinear ordinary differential equations:

$$\begin{aligned} \frac{dS}{dt} &= -\beta S(t) * I(t) + \delta R(t), \\ \frac{dE}{dt} &= \beta S(t) * I(t) - \gamma E(t), \\ \frac{dI}{dt} &= \gamma E(t) - \alpha I(t), \\ \frac{dR}{dt} &= \alpha I(t) - \delta R(t). \end{aligned} \tag{2.3}$$

One can notice the additional term $\delta R(t)$ in the above System (2.3). The parameter δ captures the transmission rate from the recovered compartment to the susceptible one due to low immunity or other health issues. Pandey et al. (2020) used the classical SEIR model to predict the outbreak of COVID-19 in India during its early stages [18]. They assumed that the loss of immunity for those recovered individuals to become susceptible again.

Another classical SEIR model for COVID-19 in the Kingdom of Saudi Arabia (KSA) includes the demography (births and deaths) developed by Ben Khedher et al. (2021) [14]. The diagram of this model can be shown in Figure 2-4 as follows:

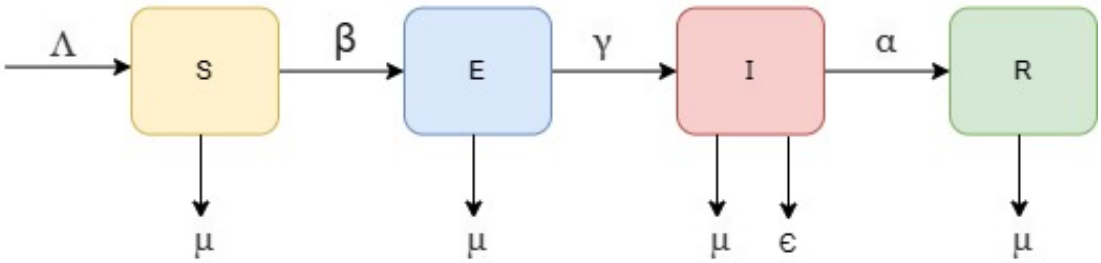

Figure 2-4: Scheme of the model SEIR studied in [14].

With the following system of nonlinear ordinary differential equations:

$$
\begin{aligned}
\frac{dS}{dt} &= \wedge - \beta S(t) * I(t) - \mu S(t), \\
\frac{dE}{dt} &= \beta S(t) * I(t) - \gamma E(t) - \mu E(t), \\
\frac{dI}{dt} &= \gamma E(t) - \alpha I(t) - \epsilon I(t) - \mu I(t), \\
\frac{dR}{dt} &= \alpha I(t) - \mu R(t).
\end{aligned}
\tag{2.4}
$$

Note that the number of ODEs formulated is four due to the number of the compartments, but the number of terms increased due to the additional three parameters, where the parameter Λ depicts the birth rate per capita, μ is the natural death rate, and ϵ is the fatality rate due to COVID-19 infection. The authors here managed to predict the dynamic of COVID-19 during a new wave after releasing all travel restrictions in KSA.

Several articles were published discussing vaccine interventions in COVID-19, testing various hypotheses, and examining different scenarios. The methodology of implementing vaccine intervention differs among the various published work. Some authors have treated the vaccine as a parameter in the SEIR model as in [19], whereas others have treated it as an additional compartment in an extended SEIR model [15, 20, 1].

The SEIR model with vaccine as a parameter in simulating the pandemic COVID-19 in Indonesia was developed by Annas et al. (2020) [19]. The diagram of the model can be shown in Figure 2-5 as follows:

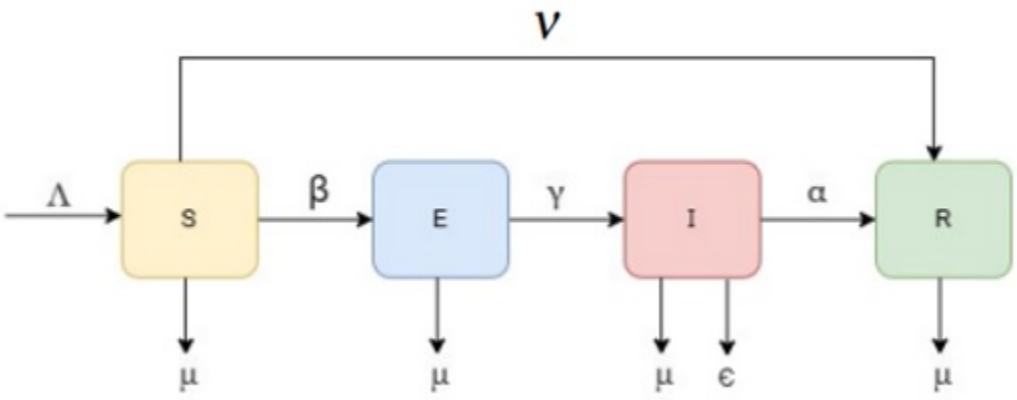

Figure 2-5: Scheme of the model SEIR studied in [19].

Where the SEIR mathematical model can be interpreted as follows:

$$\begin{aligned}
\frac{dS}{dt} &= \Lambda - \beta S(t) * I(t) - \nu S(t) - \mu S(t), \\
\frac{dE}{dt} &= \beta S(t) * I(t) - \gamma E(t) - \mu E(t), \\
\frac{dI}{dt} &= \gamma E(t) - \alpha I(t) - \epsilon I(t) - \mu I(t), \\
\frac{dR}{dt} &= \alpha I(t) + \nu S(t) - \mu R(t).
\end{aligned} \tag{2.5}$$

Again, the number of ODEs interpreting the SEIR model is four with the additional parameter ν. The parameter ν represents the percentage of the vaccinated susceptible population who gained long-life immunity and moved from the susceptible compartment to the recovered one. The authors considered the isolation and vaccination interventions as parameters in their model. They managed to gain valuable information about the global stability during COVID-19 dynamics in Indonesia as well as the prediction of the number of infected cases there. Moreover, they concluded that vaccines could speed up the COVID-19 recovery process along with isolation which could also slow COVID-19 spreading, where they both could be considered as the protection method during the early stages of the epidemic.

On the other hand, many authors implemented the vaccination intervention as an additional compartment producing an extended SEIR model. The extension is captured mathematically by adding one more ODE to the mathematical model. It is worth mentioning that these models differ from each other in terms of the hypothesis established and various inquiries and questions to be tested and answered.

Tuteja (2020) proposed an extended SEIR model, where a group of vaccinated individuals was represented as an additional compartment (V) [20]. The author investigated the stability of the model under the assumption of vaccine existence and long-life immunity. The diagram of the model can be shown in Figure 2-6 as follows:

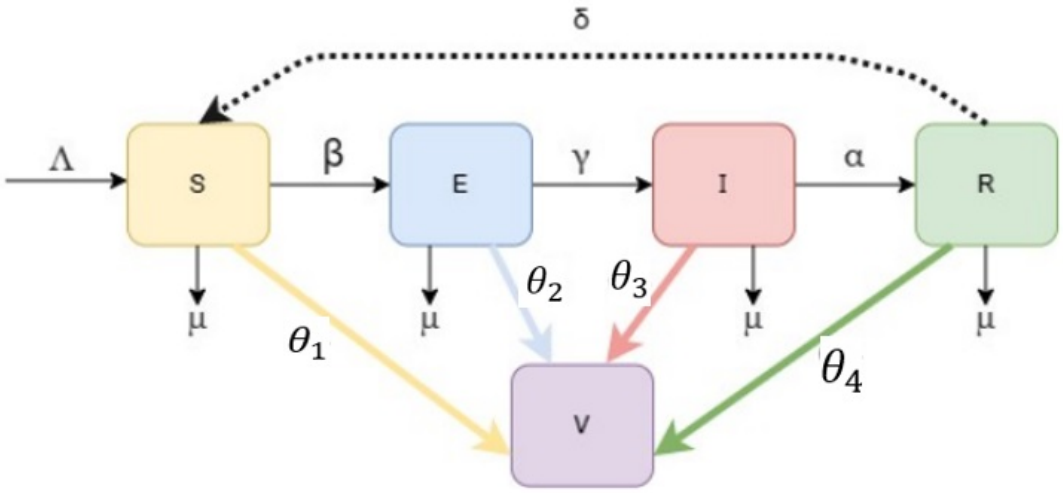

Figure 2-6: Scheme of the extended SEIR model studied in [20].

Where the extended SEIR mathematical model can be interpreted as follows:

$$\begin{aligned}
\tfrac{dS}{dt} &= \Lambda + \delta R(t) - \beta S(t) * I(t) - \theta_1 S(t) - \mu S(t),\\
\tfrac{dE}{dt} &= \beta S(t) * I(t) - \gamma E(t) - \theta_2 E(t) - \mu E(t),\\
\tfrac{dI}{dt} &= \gamma E(t) - \alpha I(t) - \theta_3 I(t) - \mu I(t),\\
\tfrac{dR}{dt} &= \alpha I(t) - \delta R(t) - \theta_4 R(t) - \mu R(t),\\
\tfrac{dV}{dt} &= \theta_1 S(t) + \theta_2 E(t) + \theta_3 I(t) + \theta_4 R(t).
\end{aligned} \tag{2.6}$$

Here we have one additional ODE for the vaccination compartment to get a total of five ODEs. The four new parameters used θ_1, θ_2, θ_3, and θ_4, represent the vaccination rates of the individuals from the susceptible, exposed, infected, and recovered compartments, respectively. The study asserted that increasing the pace of the vaccination process will help in flattening the curves of susceptible, exposed, infected, and recovered, in addition to delaying the peak period and thus lowering the fatality rate. The study was not related to a specific region or tied to real-world data but rather a general study testing hypotheses about COVID-19 disease.

Antonelli et al. (2022) suggested that individuals in the vaccination and recovered compartments would gain full-life immunity and proposed an extended SEIR model to include the vaccination and the deaths due to the infection as additional compartments [1]. They represented the infection transmission rate as a time-dependent function $\beta(t)$ in order to capture the COVID-19 dynamics precisely. Moreover, they tried to monitor

the spreading of COVID-19 and implement various scenarios of vaccination progression in Italy. The proposed model can be shown in Figure 2-7 as follows:

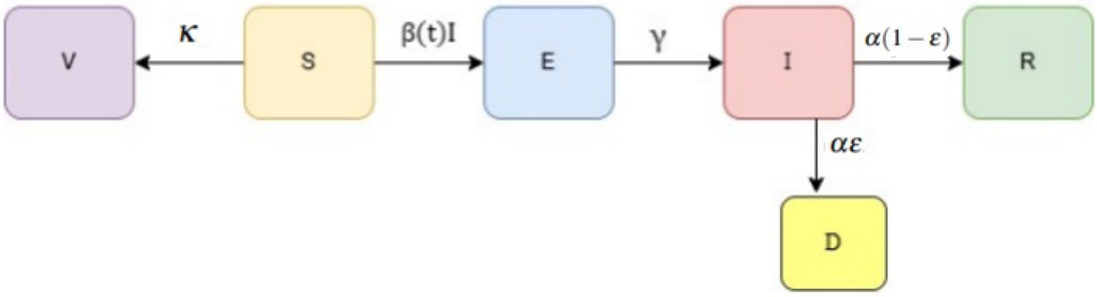

Figure 2-7: Scheme of the extended SEIR model studied in [1].

Where the extended SEIR mathematical model can be represented mathematically by the following system:

$$\begin{aligned}
\tfrac{dS}{dt} &= -\beta(t)S(t) * I(t) - \kappa S(t),\\
\tfrac{dE}{dt} &= \beta(t)S(t) * I(t) - \gamma E(t),\\
\tfrac{dI}{dt} &= \gamma E(t) - \alpha I(t),\\
\tfrac{dR}{dt} &= \alpha(1-\epsilon)I(t),\\
\tfrac{dD}{dt} &= \alpha\epsilon I(t),\\
\tfrac{dV}{dt} &= \kappa S(t).
\end{aligned} \tag{2.7}$$

Here we have two additional ODEs for the vaccination and deaths compartments to get a total of six ODEs. The authors included the parameter ϵ as a weight ($0 \leqslant \epsilon \leqslant 1$). This ϵ weight is critical in dividing the quarantined individuals into either recovered or dead with weights $1-\epsilon$ and ϵ, respectively. Therefore, the ϵ parameter depicted the proportion of dead individuals due to their personal health history or surrounding environments. They succeeded in reflecting the behavior of the COVID-19 epidemic, forecasting the spreading of infection for one month, and describing various prediction outcomes that might be derived by modeling an enhanced vaccination rate.

Ghostine et al. (2021) examined an extended SEIR model by adding three more compartments [15]. The Quarantined compartment (Q), the Deaths compartment (D),

and the Vaccination compartment (V). They studied the COVID-19 epidemic in KSA during the vaccination period. The diagram of the model can be shown in Figure 2-8 as follows:

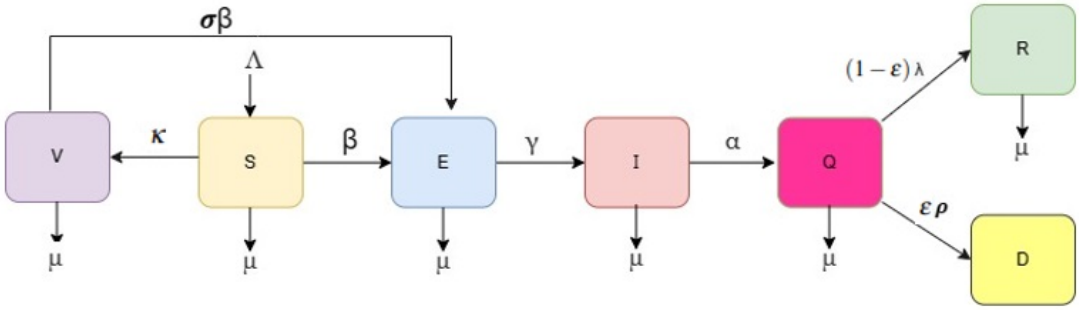

Figure 2-8: Scheme of the extended SEIR model studied in [15]

Where the extended SEIR mathematical model can be interpreted as follows:

$$\begin{aligned}
\frac{dS}{dt} &= \Lambda - \beta S(t)I(t) - \kappa S(t) - \mu S(t),\\
\frac{dE}{dt} &= \beta S(t)I(t) - \gamma E(t) + \sigma\beta V(t)I(t) - \mu E(t),\\
\frac{dI}{dt} &= \gamma E(t) - \alpha I(t) - \mu I(t),\\
\frac{dQ}{dt} &= \alpha I(t) - (1-\epsilon)\lambda Q(t) - \epsilon\rho Q(t) - \mu Q(t),\\
\frac{dR}{dt} &= (1-\kappa)\lambda Q(t) - \mu R(t),\\
\frac{dD}{dt} &= \kappa\rho Q(t),\\
\frac{dV}{dt} &= \kappa S(t) - \sigma\beta V(t)I(t) - \mu V(t).
\end{aligned} \tag{2.8}$$

There is a total of seven ODEs where each equation describes the rate of change of the population in that compartment. The researchers here used more parameters to capture more details of the epidemic. The parameters of demography were included along with other important parameters. The parameter σ is the vaccine inefficacy and takes values in [0,1]. The parameter ϵ is the case fatality rate due to infection and leads to deaths. The inverse of the parameter ρ is the average time until death. The inverse of the parameter λ is the recovery time. The inverse of the parameter α is the infection time during which the virus could be spread from the infected individual. Researchers here assumed full-life immunity for those who recovered after infection and vaccinated people may be returned to exposed ones due to the vaccine's inefficacy. They managed

to predict the COVID-19 pandemic in the KSA for two weeks and study the effectiveness of vaccination on the disease transmission.

In all of the above models, one important challenge is the model's parameters estimation and evaluation, especially for COVID-19 infectious disease, where recorded data are changing dramatically during the epidemic period. Moreover, it is widely established that COVID-19 epidemic recorded data cannot be correctly represented by any compartmental model with constant parameters throughout the whole epidemic period (Chapter 5 in [21]). We overcome this obstacle by introducing a time-dependent infection transmission rate and thus a time-dependent basic reproduction number.

In this thesis, we introduce an extension of the SEIR model that includes the vaccination and deaths as additional compartments, namely an SEIR-VD model (S: Susceptible, E: Exposed, I: Infected, R: Recovered, V: Vaccinated, and D: Deaths). We used the model to investigate the COVID-19 progression in the United Arab Emirates during the vaccination period starting from the third of July 2021 (the date on which UAE started reporting the national number of daily fully vaccinated individuals). Although vaccination in the UAE started by the end of 2020, data related to vaccination progress became publicly available as of July 2021.

Study and discuss its characteristics, and examine its stability and sensitivity. Moreover, we evaluate the basic reproduction number using the next generation method. We make some parameters to be time-dependent throughout our parameter estimation simulation. The model validation is achieved throughout the prediction period (the first two weeks of September 2021).

In the next chapter, we develop and examine the characteristics of the SEIR-VD model, including its qualitative analysis, and evaluate its basic reproduction number.

Chapter 3: SEIR-VD Epidemiological Model for COVID-19

In this chapter, we develop an SEIR-VD mathematical model (S: Susceptible, E: Exposed, I: Infectious, R: Recovered, V: Vaccinated, and D: Deaths) as a system of ODEs to investigate the COVID-19 progression assuming vaccine intervention. In addition, we analyze the general qualitative characteristics of the proposed model, such as the sensitivity analysis and the basic reproduction number R_0.

3.1 SEIR-VD Mathematical Model Assumptions

Due to the COVID-19 transmission characteristic, susceptible individuals become exposed upon contact with infected individuals before transferring to the infected compartment. The need for the exposed compartment is due to the presence of the incubation period, which represents the time that is taken for an infected individual to show symptoms and become infectious [22]. A susceptible person transfer to the exposed state after contacting the infected person due to the disease's mean incubation period, which varies from 2 to 7 days [23, 24].

Infected individuals will either recover or die depending on their health circumstances and the severity of the disease. Moreover, the vaccination process will only be applied on the susceptible individuals, and vaccinated individuals might get the infection and become exposed due to the vaccine inefficiency and contact with an infected person. Full immunity after recovery for infected individuals is not assured, depending on health history and surrounding environmental circumstances. Therefore, they might become susceptible again and get the infection through any disease transmission methods.

Before establishing the SEIR-VD model, there are specific assumptions to be followed.

- Age, sex, social status, and geo-climatic conditions are not considered in the proposed model.
- Homogeneous and uniform interaction between individuals within the community. This means that all individuals have the same rate of infection transmission in a homogeneous mixing model regardless of personal circumstances such as health conditions or age. This assumption is by default for all ODEs mathematical models.
- Demography is included, and natural births Λ and natural deaths μ are considered.

But for numerical analysis in Chapter 4, we consider a closed population without natural birth and natural death.

- The total population is constant in time, namely 'N', and it is equal to:

$$N = S(t) + E(t) + I(t) + R(t) + V(t) + D(t).$$

where N denotes the total population and the S, E, I, R, V, and D are the numbers of individuals in each compartment at any time (t).

- All parameters of the model have non-negative values.

Given the preceding assumptions, we establish the SEIR-VD mathematical model in the following section.

3.2 SEIR-VD Mathematical Model Representation

This section introduces the SEIR-VD model diagram, the system of ordinary differential equations, state variables' definitions, and the parameters.

The proposed model SEIR-VD is shown in Figure 3-1. The model diagram displays six different states of individuals (S-E-I-R-V-D), considering the loss of natural immunity δ or vaccination inefficacy σ, which will add more movements between compartments.

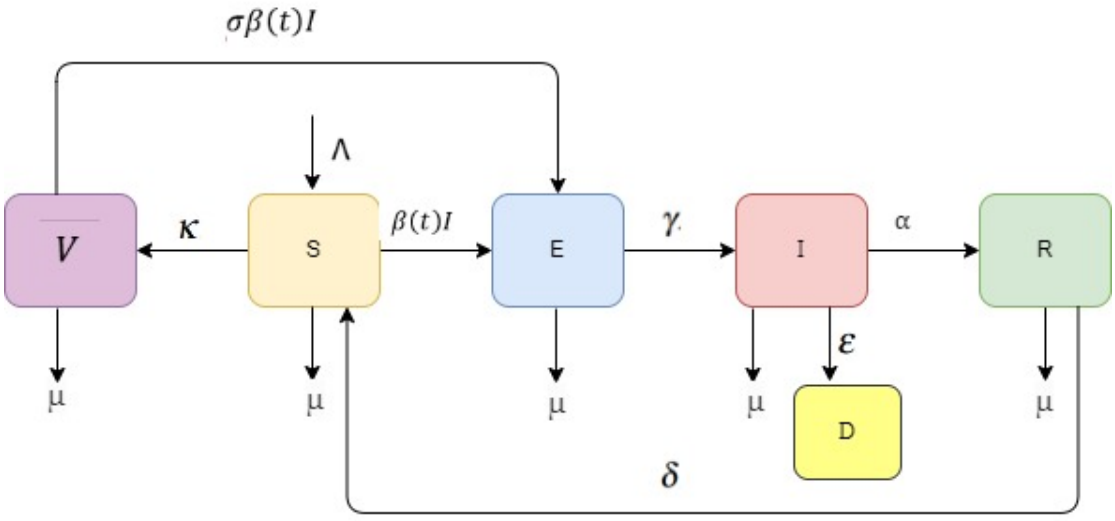

Figure 3-1: Proposed extended SEIR-VD model.

The SEIR-VD mathematical model can be represented as follows:

$$\begin{aligned}
\frac{dS}{dt} &= \Lambda + \delta R - \beta SI - \kappa S - \mu S, \\
\frac{dE}{dt} &= \beta SI + \sigma \beta VI - \gamma E - \mu E, \\
\frac{dI}{dt} &= \gamma E - \mu I - \epsilon I - \alpha I, \\
\frac{dR}{dt} &= \alpha I - \delta R - \mu R, \\
\frac{dV}{dt} &= \kappa S - \sigma \beta VI - \mu V, \\
\frac{dD}{dt} &= \epsilon I.
\end{aligned} \tag{3.1}$$

where the individuals' states (S-E-I-R-V-D) and parameters ($\delta, \beta, \kappa, \sigma, \gamma, \alpha$, and ϵ) are defined in Table (3.1) and Table (3.2) respectively.

Table 3.1: List of variables and their definitions used in the proposed model.

Variable (state)	Definition
N	Total number of populations.
S	Number of susceptible individuals as a function of time.
E	Number of exposed individuals as a function of time.
I	Number of infectious individuals as a function of time.
R	Number of recovered individuals as a function of time.
V	Number of vaccinated individuals as a function of time.
D	Number of deaths as a function of time.

Table 3.2: Parameters and their definitions in System (3.1).

Symbol	Definition
Λ	Newborn per unit of time (days).
μ	Natural death rate of S, E, I, R, and V per unit of time (days).
β	Infection transmission rate. (Indicates the expected number of infected individuals caused by an infected person per day).
γ^{-1}	Incubation period's length in days. (Average time required for exposed individuals to develop symptoms).
α^{-1}	Required time for infected individuals to recover.
ϵ	Fatality rate of the COVID-19 infected cases.
δ^{-1}	Time in days for loss of immunity after recovery caused individuals to become susceptible again.
σ	Vaccine's inefficiency rate.
κ	Vaccination rate of S compartment.

The following section includes the mathematical analysis of the SEIR-VD model. We investigate the basic reproduction number and check its sensitivity, evaluate the equilibrium points, and examine their stability. In addition, we use the next generation matrix as a method for calculating the basic reproduction number.

3.3 Mathematical Analysis of the COVID-19 SEIR-VD Model

In the following subsections, we investigate the proposed SEIR-VD model's properties, including an invariant region, equilibrium points existence, basic reproduction number ($\Re_0$), equilibrium points stability, and examine the local sensitivity of the basic reproduction number.

3.3.1 An invariant region

Here we examine the existence of solutions for System (3.1) and ensure its positive value and boundedness. We show that any solution for the system that starts with positive initial values in the first quadrant region of the coordinate plane will remain in the same quadrant for all $t \geqslant 0$. Moreover, the solution domain is bounded.

We can prove that all solutions for the SEIR-VD model with its initial conditions are

non-negative for any sub-interval of the whole domain Ω, which is defined as follows:

$$\Omega = \{(S(t), E(t), I(t), R(t), V(t), D(t)) \in R_+^6 : S(t), E(t), I(t), R(t), V(t), D(t) \geqslant 0, \forall t \in [0, \infty)\}.$$

All parameter values are non-negative: $\kappa, \beta, \sigma, \Lambda, \mu, \gamma, \alpha, \epsilon \geqslant 0$. Hence, the following statements are true:

If $S = 0 \longrightarrow \frac{dS}{dt} = \Lambda + \delta R(t) \geqslant 0$,

If $E = 0 \longrightarrow \frac{dE}{dt} = \beta S(t) I + \sigma \beta V(t) I \geqslant 0$,

If $I = 0 \longrightarrow \frac{dI}{dt} = \gamma E(t) \geqslant 0$,

If $R = 0 \longrightarrow \frac{dR}{dt} = \alpha I(t) \geqslant 0$,

If $V = 0 \longrightarrow \frac{dV}{dt} = \kappa S(t) \geqslant 0$,

If $D = 0 \longrightarrow \frac{dD}{dt} = \epsilon I(t) \geqslant 0$.

Secondly, the boundedness of the solution domain can be proven by the following argument:

At any specific time, the total population is given by:

$$N = S(t) + E(t) + I(t) + R(t) + V(t) + D(t). \tag{3.2}$$

After differentiating Equation (3.2) we get:

$$\frac{dN}{dt} = \frac{dS}{dt} + \frac{dE}{dt} + \frac{dI}{dt} + \frac{dR}{dt} + \frac{dV}{dt} + \frac{dD}{dt}. \tag{3.3}$$

In particular, $D(t) = N - (S(t) + E(t) + I(t) + R(t) + V(t))$. So, it is enough to study the following system:

$$\begin{aligned}
\tfrac{dS}{dt} &= \Lambda + \delta R - \beta S I - \kappa S - \mu S, \\
\tfrac{dE}{dt} &= \beta S I + \sigma \beta V I - \gamma E - \mu E, \\
\tfrac{dI}{dt} &= \gamma E - \mu I - \epsilon I - \alpha I, \\
\tfrac{dR}{dt} &= \alpha I - \delta R - \mu R, \\
\tfrac{dV}{dt} &= \kappa S - \sigma \beta V I - \mu V.
\end{aligned} \tag{3.4}$$

Now, we have the following value for N' using System (3.4):

$$N' = S' + E' + I' + R' + V' + D' = \Lambda - \mu(S + E + I + R + V), \tag{3.5}$$

from Equation (3.2), we have:

$$S + E + I + R + V = N - D,$$

substituting in Equation (3.5), yields:

$$N' = \Lambda - \mu(N - D) = \Lambda + \mu D - \mu N.$$

Consequently, solving the indefinite integral of the above equation with respect to time yields:

$$N(t) - D(t) = \frac{\Lambda}{\mu}(1 - e^{-\mu t}) + (N_0 - D_0)e^{-\mu t}.$$

Thus, when $t \to \infty$, we find the following inequality:

$$N(t) - D(t) \leq \frac{\Lambda}{\mu}.$$

Therefore,

$$(S(t) + E(t) + I(t) + R(t) + V(t)) \leq \frac{\Lambda}{\mu}.$$

Therefore, System (3.1) is well posed in its domain Ω from a mathematical and epidemiological point of view, where all the solutions of our proposed SEIR-VD model hold positive values for all values $0 \leqslant t < \infty$.

3.3.2 Disease free equilibrium point (DFEP)

The disease free equilibrium point is the situation when the system is free of disease and thus presumed that there is no infection. Therefore, in System (3.1), where we considered the infection compartments to be the infected and exposed, we set $I = 0$ and $E = 0$. With reference to the System (3.4), it can be reformulated as:

$$\begin{aligned}
S' &= \tfrac{dS}{dt} = \Lambda + \delta R - \beta SI - m_1 S, \\
E' &= \tfrac{dE}{dt} = \beta SI + \sigma\beta VI - m_2 E, \\
I' &= \tfrac{dI}{dt} = \gamma E - m_3 I, \\
R' &= \tfrac{dR}{dt} = \alpha I - m_4 R, \\
V' &= \tfrac{dV}{dt} = \kappa S - \sigma\beta VI - \mu V.
\end{aligned} \tag{3.6}$$

where $m_1 = \kappa + \mu$, $m_2 = \gamma + \mu$, $m_3 = \alpha + \epsilon + \mu$, $m_4 = \delta + \mu$. At the Disease free state, there are no more death due to the disease and hence 'D' state is constant. Thus, the following is true:

$$\frac{dS}{dt} + \frac{dE}{dt} + \frac{dI}{dt} + \frac{dR}{dt} + \frac{dV}{dt} = 0. \tag{3.7}$$

Therefore, the DFEP for System (3.6) is given by $(S^*, E^*, I^*, R^*, V^*)$, where

$$S^* = \frac{\Lambda}{(\kappa + \mu)}, \quad E^* = 0, \quad I^* = 0, \quad R^* = 0, \quad V^* = \frac{\kappa\Lambda}{\mu(\kappa + \mu)}. \tag{3.8}$$

and the number of deaths D^* at the DFEP expressed as $D^* = N - S^* - V^*$. Hence, there exists a disease free equilibrium point (DFEP=P_0):

$$P_0 = (S^*, E^*, I^*, R^*, V^*) = (\frac{\Lambda}{(\kappa + \mu)}, 0, 0, 0, \frac{\kappa\Lambda}{\mu(\kappa + \mu)}). \tag{3.9}$$

3.3.3 Endemic equilibrium point (EEP)

The endemic equilibrium point (EEP) is when the disease persists within the community. Solving the system in Equation (3.6) to find the EEP by evaluating the following equations:

$$\frac{dS}{dt} = \Lambda + \delta R - \beta sI - m_1 S = 0. \tag{3.10}$$

$$\frac{dE}{dt} = \beta SI + \sigma\beta VI - m_2 E = 0. \tag{3.11}$$

$$\frac{dI}{dt} = \gamma E - m_3 I = 0. \tag{3.12}$$

$$\frac{dR}{dt} = \alpha I - m_4 R = 0 \tag{3.13}$$

$$\frac{dV}{dt} = \kappa S - \sigma\beta VI - \mu V = 0. \tag{3.14}$$

From Equation (3.10) we get $S(\beta I + m_1) = \Lambda + \delta r$ then $S^* = \frac{\Lambda + \delta R^*}{\beta I + m_1} = \frac{\Lambda m_4 + \delta\alpha I}{m_4(\beta I + m_1)}$.

From Equation (3.12) we get $\gamma e = m_3 I$ then $E^* = \frac{m_3}{\gamma} I$.

From Equation (3.13) we get $\alpha I = m_4 R$ then $R^* = \frac{\alpha}{m_4} I$.

Add both Equations (3.11) and (3.14) yields:

$$\beta SI + \kappa S - m_2 E - \mu V = 0.$$

After substituting the values of E^* and S^* we get:

$$\beta\frac{\Lambda m_4+\delta\alpha I}{m_4(\beta I+m_1)}I+\kappa\frac{\Lambda m_4+\delta\alpha I}{m_4(\beta I+m_1)}-m_2\frac{m_3}{\gamma}I-\mu V=0,$$

$$\beta\frac{\Lambda m_4+\delta\alpha I}{m_4(\beta I+m_1)}I+\kappa\frac{\Lambda m_4+\delta\alpha I}{m_4(\beta I+m_1)}-m_2\frac{m_3}{\gamma}I=\mu V,$$

$$V^*=\frac{\gamma\beta\Lambda m_4 I+\sigma\beta I(\beta\Lambda\gamma I+\kappa\Lambda\gamma-m_2m_3I(\beta I+m_1))-m_2m_3I\mu(\beta I+m_1)}{\gamma\mu m_4(\beta I+m_1)}.$$

Substituting the values of V^* and S^* and E^* in Equation (3.11) yields the quadratic equation for I^*:

$$b_1(I^*)^2+b_2I^*+b_3=0. \tag{3.15}$$

where:

$b_1=m_2m_3\beta^2\sigma$,

$b_2=m_1m_2\beta\mu+m_1m_2m_3\beta\sigma-\beta^2\gamma\Lambda\sigma$, and

$b_3=m_1m_2m_3m_4\mu-m_4\beta\gamma\Lambda\mu-m_4\beta\gamma\Lambda k\sigma$.

Manipulating the formula of b_3 using the evaluated $\Re_0$ as shown in the Equation (3.17) in the coming subsection (3.3.5), $\Re_0=\frac{\gamma\beta\Lambda(\mu+\sigma\kappa)}{\mu(\mu+\gamma)(\mu+\epsilon+\alpha)(\mu+\kappa)}$, hence we can rewrite the b_3 as follows:

$$b_3=1-\Re_0.$$

Evaluating the roots of the second order characteristic Equation (3.15):

$$\frac{-b_2\pm\sqrt{(b_2^2-4b_1b_3)}}{2b_1}.$$

where we have $b_3<0$ ($\Re_0>1$), there will be a positive root($I^*>0$). Hence, the EEP exists at $P^*=(S^*,E^*,I^*,R^*,V^*)$, where we have positive values for all states (variables).

3.3.4 The basic reproduction number is calculated using the next generation matrix (NGM) method

It is critical in epidemiology to quantify the severity of the infectious disease. The standard procedure is to compute so-called the basic reproduction number ($\Re_0$), which

characterizes the epidemic occurrence due to an outbreak's potential. $\Re_0$ is a measure used in epidemiology to describe the contagiousness or risk of transmission of infectious pathogens as defined by the Centers for Disease Control and prevention (CDC), USA [25]. It has been widely used to assess pathogen transmissibility, outbreak severity, and epidemiological control. $\Re_0$ definition has been established by Anderson and May (1992) as: *"the average number of secondary infections produced when one infected individual is introduced into a host population where everyone is susceptible"* [26].

It is a threshold parameter that determines whether or not an outbreak will result in an epidemic. If $\Re_0 < 1$, then a few infected individuals introduced into a completely susceptible population will, on average, fail to replace themselves, and the disease will not spread [27]. This means that infection cannot take off where disease dies off, and no outbreak exists. On the other hand, if $\Re_0 > 1$, then the number of infected individuals will increase with each generation, and the disease will spread. Wherein the epidemic or outbreak exists in a population. And if $\Re_0 = 1$, then the disease will be endemic.

There are several methods for computing this critical quantity ($\Re_0$). One method employs the Jacobian matrix of the ODEs of the model. It works well, especially for simple or classical models such as SIR or SEIR models. However, mathematical models become more complex when adding more compartments, especially in infected compartments such as asymptomatic and symptomatic, to better capture the disease dynamic. In that case, the Jacobian matrix method is challenging because it depends on the algebraic Routh-Hurwitz conditions for the Jacobian matrix stability. In particular, this method depends on finding the eigenvalues' character of the matrix of the linearized system associated with a system of non-linear ODEs. Where we have to trace the positive real parts of the roots of a real algebraic equation [28].

An alternative method is the next generation matrix (NGM) method. It is suitable for extension models where complexity exists. The NGM method is proposed by Diekmann et al. (1990) [29], and elaborated by Van den Driessche and Watmough (2002) [30].

In this section, we use the next generation method as presented in [31] to compute the basic reproduction. We decompose the six compartments into two main categories where we have compartments containing the pathogen-carrying individuals (E and I), and the others disease-free individuals (S, R, V, and D).

In particular, for $x \in R^2_+$, where $x := (x_1, x_2) = (E, I)$, and $y \in R^4_+$ where

$y = (y_1, \ldots, y_4) = (S, R, V, D)$ are sub-populations in infected and non infected compartments, respectively.

Then we define $\mathcal{F}_i$ and $\mathcal{V}_j$ as functions or operators of higher dimensional space where $\mathcal{F}_i$ indicates increasing (gain) of secondary infection rate in the i^{th} compartment, and $\mathcal{V}_i$ indicates decreasing (loss) of the secondary infection rate in the i^{th} compartment by death or recovery. $\mathcal{V}_i^+(x)$ indicates the transfer rate into compartment i from other compartments, and $\mathcal{V}_i^-(x)$ is the transfer rate out of compartment i. Our original system can be written as:

$$\frac{dx_i}{dt} = \mathcal{F}_i(x, y) - \mathcal{V}_i(x, y), \quad i = 1, 2, \qquad where \qquad \mathcal{V}_i = \mathcal{V}_i^- - \mathcal{V}_i^+,$$

$$\frac{dy_j}{dt} = g_j(x, y), \quad j = 1, 2, 3, 4.$$

We could linearize the equations around the disease free equilibrium point (DFEP) of disease compartments x, which gives:

$$\frac{dx_i}{dt} = (F - V)x.$$

where F and V with respect to the infected compartments (E and I):

$$F_{ij} = \frac{\partial \mathcal{F}_i}{\partial x_j}(0, y_0).$$

and

$$V_{ij} = \frac{\partial \mathcal{V}_i}{\partial x_j}(0, y_0).$$

Then, we define a matrix K of $(2x2)$ dimension to be called the Next Generation Matrix.

$$K = FV^{-1}.$$

Where k_{ij} entry indicates the number of newly infected individuals in compartment i that is generated by currently infected individuals in compartment j during a specific period (n).

Assume that n is the time required for the infected individuals (within disease compart-

ments E and I) to develop themselves in generation can be modeled in a matrix form, and x is a vector of dimension two as follows:

$$x(n+1) = Kx(n). \tag{3.16}$$

Thus the basic reproduction number $\Re_0$ is found to be the spectral radius of the NGM (K)which is the eigenvalue with maximum modulus in the spectrum of K and given by:

$$\Re_0 = \rho(K).$$

3.3.5 The basic reproduction number of our model and its role in disease free equilibrium point stability

Using the NGM to evaluate the basic reproduction number $\Re_0$ during vaccine intervention for the system in Equation (3.1) by employing the fundamentals of NGM as follows:

Let the infected compartments be (E) and (I) and $\frac{dX}{dt} = \mathcal{F} - \mathcal{V}$ where:

$$\frac{dX}{dt} = \begin{bmatrix} \frac{dE}{dt} \\ \frac{dI}{dt} \end{bmatrix}, \mathcal{F} = \begin{bmatrix} \beta SI + \sigma\beta VI \\ 0 \end{bmatrix}, \mathcal{V} = \begin{bmatrix} \gamma E + \mu E \\ -\gamma E + \mu I + \epsilon I + \alpha I \end{bmatrix}.$$

Therefore, evaluating the Jacobian matrices of $\mathcal{F}$ and $\mathcal{V}$ at the DFEP will yield:

$$F = \begin{bmatrix} 0 & \beta S^* + \sigma\beta V^* \\ 0 & 0 \end{bmatrix}, \quad V = \begin{bmatrix} \mu + \gamma & 0 \\ -\gamma & \mu + \epsilon + \alpha \end{bmatrix},$$

$$V^{-1} = \frac{1}{(\mu+\gamma)(\mu+\epsilon+\alpha)} \begin{bmatrix} \mu + \epsilon + \alpha & 0 \\ \gamma & \mu + \gamma \end{bmatrix},$$

$$K = FV^{-1} = \frac{1}{(\mu+\gamma)(\mu+\epsilon+\alpha)} \begin{bmatrix} \gamma(\beta S^* + \sigma\beta V^*) & (\mu+\gamma)(\beta S^* + \sigma\beta V^*) \\ 0 & 0 \end{bmatrix}.$$

where S^* and V^* is defined at the DFEP from Equation (3.8) Then, the spectral radius of the NGM K will be $\Re_0$:

$$\Re_0 = \rho\left(FV^{-1}\right) = \frac{\gamma(\beta S^* + \sigma\beta V^*)}{(\mu+\gamma)(\mu+\epsilon+\alpha)} = \frac{\gamma\beta(S^* + \sigma V^*)}{(\mu+\gamma)(\mu+\epsilon+\alpha)},$$

$$\Re_0 = \frac{\gamma\beta(S^* + \sigma V^*)}{(\mu+\gamma)(\mu+\epsilon+\alpha)},$$

Substituting the values of s^* and v^* yields:

$$\Re_0 = \frac{\gamma\beta\Lambda(\mu+\sigma\kappa)}{\mu(\mu+\gamma)(\mu+\epsilon+\alpha)(\mu+\kappa)}, \tag{3.17}$$

The assumption $\Lambda = \mu$ yields that:

$$\Re_0 = \frac{\gamma\beta(\mu+\sigma\kappa)}{(\mu+\gamma)(\mu+\epsilon+\alpha)(\mu+\kappa)}, \tag{3.18}$$

In case of $\sigma = 0$, our SEIR-VD model will be reduced to the SEIRS model without vaccination [32]. Where we consider the basic reproduction number to be:

$$\Re_0 = \frac{\beta\gamma}{(\mu+\gamma)(\mu+\epsilon+\alpha)}, \tag{3.19}$$

And under negligible natural deaths ($\mu \approx 0$) yields:

$$\Re_0 = \frac{\beta}{\alpha+\epsilon}. \tag{3.20}$$

We can interpret the basic reproduction number during the vaccination process shown in Equation (3.18) as follows: A fraction of those individuals who have been in the exposed compartment $\frac{\gamma}{\mu+\gamma}$ progress and transfer to the infection compartment before dying; while the fraction $\frac{1}{\mu+\epsilon+\alpha}$ represents the number of secondary infections caused by one infective individual during his/her infectious period. The last fraction $\frac{\mu+\sigma\kappa}{\mu+\kappa}$ depicts the vaccine effects on the secondary infections where we can note that if σ =1 (vaccine efficiency is 0) yields no effect of the vaccine on the disease dynamic (useless). While in the case of σ=0 the fraction will decrease the disease spreading by a fraction of ($\frac{\mu}{\mu+\kappa}$). Therefore, the average vaccinated individuals with vaccination rate κ have contributed to the fraction $\frac{\gamma\beta(\mu+\sigma\kappa)}{(\mu+\gamma)(\mu+\epsilon+\alpha)(\mu+\kappa)}$ of the secondary infection.

Stability analysis for the disease free equilibrium point and the existence of the endemic equilibrium point using the $\Re_0$ formula:

a) The DFEP stability analysis:

Evaluating the Jacobian matrix for the system of Equation (3.6) at the disease free equilibrium point (3.9).

First, the Jacobian matrix:

$$J(S,E,I,R,V) = \begin{pmatrix} -m_1-\beta I & 0 & -\beta S & \delta & 0 \\ \beta I & -m_2 & \beta S+\beta\sigma V & 0 & \beta\sigma I \\ 0 & \gamma & -m_3 & 0 & 0 \\ 0 & 0 & \alpha & -m_4 & 0 \\ K & 0 & -\beta\sigma V & 0 & -\mu-\beta\sigma I \end{pmatrix}. \tag{3.21}$$

Then, evaluating the Jacobian matrix at the DFEP (3.9) yields:

$$J(S,E,I,R,V)_{(S^*,0,0,0,V^*)} = \begin{pmatrix} -m_1 & 0 & -\beta S^* & \delta & 0 \\ 0 & -m_2 & \beta S^*+\beta\sigma V^* & 0 & 0 \\ 0 & \gamma & -m_3 & 0 & 0 \\ 0 & 0 & \alpha & -m_4 & 0 \\ K & 0 & -\beta\sigma V^* & 0 & -\mu \end{pmatrix}, \tag{3.22}$$

Substituting the values of S^* and V^* from the Equation (3.9) in the System (3.22), where $S^* = \frac{\Lambda}{m_1}$ and $V^* = \frac{\kappa\Lambda}{\mu(m_1)}$ gives:

$$J(S,E,I,R,V)_{(S^*,0,0,0,V^*)} = \begin{pmatrix} -m_1 & 0 & -\frac{\beta\Lambda}{m_1} & \delta & 0 \\ 0 & -m_2 & \frac{\beta\Lambda}{m_1}+\frac{\beta K\Lambda\sigma}{m_1\mu} & 0 & 0 \\ 0 & \gamma & -m_3 & 0 & 0 \\ 0 & 0 & \alpha & -m_4 & 0 \\ K & 0 & -\frac{\beta K\Lambda\sigma}{m_1\mu} & 0 & -\mu \end{pmatrix}. \tag{3.23}$$

Find the determinant of the following system: $\left|J(S,E,I,R,V)_{(S^*,0,,0,0,V^*)} - I\lambda\right| = 0$, yields:

$$\begin{vmatrix} -m_1-\lambda & 0 & -\frac{\beta\Lambda}{m_1} & \delta & 0 \\ 0 & -m_2-\lambda & \frac{\beta\Lambda}{m_1}+\frac{\beta K\Lambda\sigma}{m_1\mu} & 0 & 0 \\ 0 & \gamma & -m_3-\lambda & 0 & 0 \\ 0 & 0 & \alpha & -m_4-\lambda & 0 \\ K & 0 & -\frac{\beta K\Lambda\sigma}{m_1\mu} & 0 & -\mu-\lambda \end{vmatrix} = 0, \tag{3.24}$$

Solving the System (3.24), yields the following characteristic polynomial equation:

$$-\frac{(m1+\lambda)(m4+\lambda)(\lambda+\mu)(m1(m2+\lambda)(m3+\lambda)\mu-\beta\gamma\Lambda(\mu+K\sigma))}{m1\mu}=0,$$

Hence, the eigenvalues are: $\lambda_1 = -m_1 \leqslant 0$, $\lambda_2 = -m_4 \leqslant 0$, $\lambda_3 = -\mu \leqslant 0$, and the remaining λ_4 and λ_5 will be the roots of the Quadratic in Lambda:

$$-\frac{(m_1(m_2+\lambda)(m_3+\lambda)\mu-\beta\gamma\Lambda(\mu+K\sigma))}{m_1\mu}=0,$$

With the characteristic equations:

$$-\lambda^2-\lambda\frac{(\mathrm{m1}m_2\mu+m_1m_3\mu)}{m_1\mu}-\frac{m_1m_2m_3\mu-\beta\gamma\Lambda(\mu+\mathrm{K}\sigma)}{m_1\mu}=0, \tag{3.25}$$

After manipulating to get $\Re_0$ formula within characteristic equation of λ yields:

$$-\frac{\lambda^2}{m_2m_3}-\frac{\lambda(m_1m_2\mu+m_1m_3\mu)}{m_1m_2m_3\mu}-\frac{m_1m_2m_3\mu-\beta\gamma\Lambda(\mu+K\sigma)}{m_1m_2m_3\mu}, \tag{3.26}$$

substituting the $\Re_0$ formula in Equation (3.17) yields:

$$\frac{\lambda^2}{m_2m_3}+\lambda\frac{(m_1m_2\mu+m_1m_3\mu)}{m_1m_2m_3\mu}+(1-\Re_0)=0, \tag{3.27}$$

Then, we have:

$$\lambda^2+\lambda\frac{m_2m_3(m_1m_2\mu+m_1m_3\mu)}{m_1\mu}+m_2m_3(1-\Re_0)=0. \tag{3.28}$$

Applying the trace-determinant ($T-D$) stability analysis, we get the following, let: $T=-\frac{m_2m_3(m_1m_2\mu+m_1m_3\mu)}{m_1\mu}$, and $D=m_2m_3(1-\Re_0)$. Then the eigenvalues will be:

$$\lambda_4 = \frac{T + \sqrt{T^2 - 4D}}{2}, \tag{3.29}$$

$$\lambda_5 = \frac{T - \sqrt{T^2 - 4D}}{2}. \tag{3.30}$$

Hence, the $T < 0$ and the $D > 0$ if and only if the $\Re_0 < 1$, consequently the eigenvalues λ_4 and λ_5 will lead to a stable system of either two choices:

1. Both eigenvalues are complex with negative real parts.
2. Both eigenvalues are real and hold negative values.

Thus, the DFEP exists and is stable.

a) The EEP existence:

Manipulating the formula of b_3 in Equation (3.15) using the evaluated $\Re_0$ as shown in the Equation (3.17), $\Re_0 = \frac{\gamma\beta\Lambda(\mu+\sigma\kappa)}{\mu(\mu+\gamma)(\mu+\epsilon+\alpha)(\mu+\kappa)}$, hence we can rewrite the b_3 as follows:

$$b_3 = 1 - \Re_0.$$

It is clear that: $b_3 < 0$ if $(1 - \Re_0) < 0$ then $\Re_0 > 1$, therefore the Equation (3.15) has a unique positive root and the endemic equilibrium point exists $P^* = (S^*, E^*, I^*, R^*, V^*)$.

3.3.6 Local sensitivity analysis of the basic reproduction number ($\Re_0$)

The parameters used in the mathematical model for infectious diseases have essential effects on the basic reproduction number ($\Re_0$). After evaluating these parameters via fitting, we can investigate the critical role of the $\Re_0$. Significantly, the effect of changing one parameter such as p on that critical epidemiological indicator ($\Re_0$) is written as:

$$S^p_{\Re_0} = \frac{\partial \Re_0}{\partial p}. \tag{3.31}$$

This method is called the local sensitivity analysis due to the assumption that all parameters are retained at their estimated values, including the parameter p ([33]-chapter6).

However, although this method doesn't consider the simultaneous variation of all parameters, it is highly influenced by the magnitude of p and the value of $\Re_0$. Therefore, a better indicator would be the elasticity of $\Re_0$ to p. Which is defined as the percentage change of the $\Re_0$ quantity due to the percentage change of the magnitude of parameter

p. The elasticity concept is written as:

$$\varepsilon^{p}_{\Re_0} = (\frac{\partial \Re_0}{\partial p})(\frac{p}{\Re_0}) \approx \pm \frac{\%\Delta \Re_0}{\%\Delta p}. \tag{3.32}$$

The sign of the elasticity depicts the behavior of the $\Re_0$. When the elasticity is positive, it reflects the increment of $\Re_0$ with respect to p. On the other hand, when it is negative, it reflects the decrements of $\Re_0$ with respect to p. In particular, positive sensitivity parameters reflect that there is a positive effect on the increment of the basic reproduction number ($\Re_0$). Thus, increasing or decreasing the specified parameter while keeping the other parameters constant will result in increasing or decreasing the basic reproduction number ($\Re_0$) respectively. Negative sensitivity parameters reflect that there is a negative effect on the increment of the basic reproduction number ($\Re_0$).

We apply here the last equation of the evaluated $\Re_0$ for the SEIR-VD model as in Equation (3.18) to study the elasticity with respect to each parameter individually. Recall equation $\Re_0$ is given by:

$$\Re_0 = \frac{\gamma\beta(\mu + \sigma\kappa)}{(\mu + \gamma)(\mu + \epsilon + \alpha)(\mu + \kappa)}.$$

Then, the local elasticity of the $\Re_0$ with respect to the vaccination inefficiency (σ) is:

$$\varepsilon^{\sigma}_{\Re_0} = (\frac{\partial \Re_0}{\partial \sigma})(\frac{\sigma}{\Re_0}),$$

Then:

$$\varepsilon^{\sigma}_{\Re_0} = \left(\frac{\gamma\beta\kappa}{(\mu + \gamma)(\mu + \epsilon + \alpha)(\mu + \kappa)}\right)\left(\frac{\sigma(\mu + \gamma)(\mu + \epsilon + \alpha)(\mu + \kappa)}{\gamma\beta(\mu + \sigma\kappa)}\right),$$

Hence:

$$\varepsilon^{\sigma}_{\Re_0} = \frac{\sigma\kappa}{\sigma\kappa + \mu} > 0. \tag{3.33}$$

Thus the higher value of the vaccine's efficiency (lower the σ value of the vaccine's inefficiency) will cause a decrement in $\Re_0$. Where vaccinated individuals are immunized and can't be infected, decreasing the transmission rate of disease in the community. Where the positive value means that the decrement in σ (efficient vaccine) will cause a decrement in the $\Re_0$.

The local elasticity of the $\Re_0$ with respect to the vaccination rate (κ) can be evaluated by:

$$\varepsilon_{\Re_0}^{\kappa} = (\frac{\partial \Re_0}{\partial \kappa})(\frac{\kappa}{\Re_0}),$$

Then:

$$\left(\frac{\beta\gamma\sigma}{(\gamma+\mu)(\alpha+\varepsilon+\mu)(\alpha+\mu)} - \frac{\beta\gamma(\chi\sigma+\mu)}{(\gamma+\mu)(\alpha+\varepsilon+\mu)(\kappa+\mu)^2}\right)\left(\frac{\kappa(\mu+\gamma)(\mu+\epsilon+\alpha)(\mu+\kappa)}{\gamma\beta(\mu+\sigma\kappa)}\right),$$

After simplifying yields:

$$\varepsilon_{\Re_0}^{\kappa} = \frac{\kappa(-1+\sigma)\mu}{(\kappa+\mu)(\kappa\sigma+\mu)} < 0. \tag{3.34}$$

Here, under the assumption that all parameters are non-negative, and $0 < \sigma < 1$, the value of $\varepsilon_{\Re_0}^{\kappa}$ is negative. The interpretation of the disease dynamic is that the higher the rate of vaccination, the lower value of $\Re_0$, which means the more vaccination progression the lower spreading disease will be, and on the other hand, the lower the vaccination rate, the more spreading of disease will be.

The local elasticity of the $\Re_0$ with respect to the transmission rate from susceptible individuals to exposed (β) can be evaluated by:

$$\varepsilon_{\Re_0}^{\beta} = (\frac{\partial \Re_0}{\partial \beta})(\frac{\beta}{\Re_0}),$$

Then:

$$\varepsilon_{\Re_0}^{\beta} = \left(\frac{\gamma(\kappa\sigma+\mu)}{(\gamma+\mu)(\alpha+\varepsilon+\mu)(\kappa+\mu)}\right)\left(\frac{\beta(\mu+\gamma)(\mu+\epsilon+\alpha)(\mu+\kappa)}{\gamma\beta(\mu+\sigma\kappa)}\right),$$

After simplifying yields:

$$\varepsilon_{\Re_0}^{\beta} = 1 > 0. \tag{3.35}$$

This indicates that an increment of 1% in β value will cause a 1% rise in $\Re_0$. Thus, the transmission rate increment will cause an increment in the $\Re_0$ and the transmission rate decrements will cause decrements in the $\Re_0$.

The local elasticity of the $\Re_0$ with respect to the transmission rate from exposed individuals to infected (γ) can be evaluated by:

$$\varepsilon^{\gamma}_{\Re_0} = (\frac{\partial \Re_0}{\partial \gamma})(\frac{\gamma}{\Re_0}),$$

Then:

$$\varepsilon^{\gamma}_{\Re_0} = \left(\frac{\beta\mu(\kappa\sigma+\mu)}{(\gamma+\mu)^2(\alpha+\varepsilon+\mu)(\kappa+\mu)}\right)\left(\frac{\gamma(\mu+\gamma)(\mu+\epsilon+\alpha)(\mu+\kappa)}{\gamma\beta(\mu+\sigma\kappa)}\right),$$

After simplifying yields:

$$\varepsilon^{\gamma}_{\Re_0} = \frac{\mu}{\gamma+\mu} > 0. \tag{3.36}$$

The value of γ is the inverse of the incubation period (transmission rate from E compartment to I compartment). The increment of the value of transmission rate from E compartment to I compartment (lower incubation period) will produce a higher disease spreading in the community and thus a rise in $\Re_0$.

The local elasticity of the $\Re_0$ with respect to the transmission rate from infected individuals to recovered (α) can be evaluated by:

$$\varepsilon^{\alpha}_{\Re_0} = (\frac{\partial \Re_0}{\partial \alpha})(\frac{\alpha}{\Re_0}),$$

Then:

$$\varepsilon^{\alpha}_{\Re_0} = \left(-\frac{\beta\gamma(\kappa\sigma+\mu)}{(\gamma+\mu)(\alpha+\varepsilon+\mu)^2(\kappa+\mu)}\right)\left(\frac{\alpha(\mu+\gamma)(\mu+\epsilon+\alpha)(\mu+\kappa)}{\gamma\beta(\mu+\sigma\kappa)}\right),$$

After simplifying yields:

$$\varepsilon^{\alpha}_{\Re_0} = \frac{-\alpha}{\alpha+\epsilon+\mu} < 0. \tag{3.37}$$

The value of α is the inverse of the recovery period (transmission from I compartment to R compartment). So the higher α value (lower recovery period), which means the fastest movement from I compartment to R compartment and thus the individuals become immunized, which will affect the disease spreading negatively and cause a reduction in the $\Re_0$ value and on the other hand the lower value of α will yield to an increment in $\Re_0$.

The local elasticity of the $\Re_0$ with respect to the fatality rate (ϵ) (deaths due to

COVID-19) can be evaluated by

$$\varepsilon^{\epsilon}_{\Re_0} = (\frac{\partial \Re_0}{\partial \epsilon})(\frac{\epsilon}{\Re_0}),$$

Then:

$$\varepsilon^{\epsilon}_{\Re_0} = \left(-\frac{\beta\gamma(\kappa\sigma+\mu)}{(\gamma+\mu)(\alpha+\varepsilon+\mu)^2(\kappa+\mu)}\right)\left(\frac{\epsilon(\mu+\gamma)(\mu+\epsilon+\alpha)(\mu+\kappa)}{\gamma\beta(\mu+\sigma\kappa)}\right),$$

After simplifying yields:

$$\varepsilon^{\epsilon}_{\Re_0} = \frac{-\epsilon}{\alpha+\epsilon+\mu} < 0. \tag{3.38}$$

The value of ϵ indicates the fatality rate of COVID-19. If the number of deaths increases due to the higher fatality rate, there will be no more susceptible individuals to be infected, thus affecting the disease spreading negatively. Therefore, the $\Re_0$ will decrease accordingly.

The value of elasticity is critical in affecting the attitude of the basic reproduction number ($\Re_0$) of the model. Where we can note from Equations (3.33) to (3.38) some have negative values while others have positive values, which means changing a one specified parameter while keeping the other parameters constant may result in changing the basic reproduction number $\Re_0$ and hence the infection dynamic of the disease.

In the next chapter, we investigate the numerical analysis and results of the proposed model.

Chapter 4: The UAE Case Study: Numerical Analysis and Curve Fitting

4.1 Introduction

The underlying assumption in solving the ODEs compartmental models is that the system's parameters are inherently constant. However, this might not be the case in simulating infectious disease dynamics over a specific time interval. The variability of those parameters must be captured properly due to various justifications such as external environmental factors that directly affect the disease's spread over time. Generally, parameters represent some epidemiological characteristics related to the disease progression. The dynamic of any infectious disease is highly affected by various interventions such as vaccination and social behavior rules and regulations. Consequently, the parameters will ultimately vary with the variation in the surrounding environment.

The treatment of varying time-dependent parameters has been employed in various studies in the literature. For example, the infection transmission rate β has been defined as a periodic function to be able to capture the seasonality of the influenza epidemic (Chapter 5 in [21]). The resulting model is termed "forced" model. Another example is an Ebola outbreak model, which used β as an exponential function in time [34]. Recently, several authors proposed many time-dependent parameters in studying COVID-19 progression and investigating the various control scenarios and multi-scale epidemics [35, 36]. Other modified SEIR compartmental models with the adoption of the non-constant (time-dependent) infection rate β were implemented to monitor and control the COVID-19 dynamics under specific interventions [13, 1, 37].

Therefore, the external environmental circumstances such as the new government's restrictions and rules for disease precautions, the daily recorded data, particularly the number of infected individuals, vary to a significant extent. For our UAE case study, for example, around mid of August 2021, most of the educational institutions and other private and governmental sectors in the UAE started in-person attendance. Consequently, the dynamic of COVID19 changed, causing a change in the epidemiological parameters.

In this chapter, we employ time-dependent parameters $(\gamma, \beta, \alpha, \epsilon, \kappa, \sigma)$ to produce a realistic epidemic view and forecast COVID-19 dynamics. Thus, the basic reproduction number $\Re_0$, which is directly proportional to the infection transmission rate β, also becomes a time-dependent quantity.

In the next section, we estimate the parameters and calibrate the proposed model

over the whole interval considered in this study, [July 3-August 31, 2021].

4.2 Tools, Model Assumptions, and Calibrations

The graphical and numerical produced in this thesis are obtained by employing the required algorithms using the MATLAB programming language software version R2021a via Intel core i7-10th generation processor.

The model's curve-fitting problem is achieved by solving the time series of data in Appendix B acquired by the FCSC [38]. Fourth Order-Runge Kutta method is used to solve the differential equations in the System (3.1) over successive sub-intervals. We solved a sequence of constrained minimization problems to minimize residuals-based objective function with bounded parameters. The least-squares method is used to optimize the residuals between the model's predicted data and the recorded data. The non-linear curve fitting solver "lsqnonlin" from MATLAB tools is used for this purpose.

The system defined in Equation (3.1) excluding the demography (natural death μ and birth Λ), is manipulated under the following assumptions and conditions for parameter estimation and model calibration:

- The loss of immunity after recovery is very low ($\delta \approx 0$).
- The vaccination provides 100% immunity($\sigma \approx 0$).
- Formulating the function $q(t)$ by employing a linear interpolating function for the vaccination recorded database.

The equation of the vaccination state is represented as q(t), and the finite backward difference of $\frac{dV}{dt}$ is represented from recorded vaccination data. The $\frac{dV}{dt}$ can be expressed as follows:

$$\frac{dV}{dt} = q(t) = \begin{cases} V_i - V_{i-1}, & i = 2, ..., n \quad \text{where } n \text{ is the number of days,} \\ 0, & i = 1. \end{cases} \tag{4.1}$$

Initial value of 0 on the first day for the purpose of adjusting the dimension of backward difference. Since $q(t) = \kappa S$. Therefore, κ is calculated as a fraction of the total number of vaccinated individuals to the total number of susceptible individuals.

4.3 Parameter Estimation and Model Calibration Over the Whole Interval

In this section, we apply our numerical analysis for the proposed model using the UAE during vaccination intervention as a case study. Data is used from the official website of the Federal Competitiveness and Statistical Center (FCSC) [38]
Recall our proposed nonlinear ODEs system of the SEIR-VD model from Equation (3.1) excluding the demography (natural death μ and birth Λ) with the following initial conditions of the states represented as follows:

$$S(t_0) = S_0, \quad E(t_0) = E_0, \quad I(t_0) = I_0, \quad R(t_0) = R_0, \quad V(t_0) = V_0, \quad D(t_0) = D_0. \tag{4.2}$$

All states are available except for S_0 and E_0. The initial value of the E_0 can be evaluated using the following formula:

$$E(t_0) = \sum_{t=t_0}^{t=t_0+t_{avg}} I_{n_t}. \tag{4.3}$$

where I_{n_t} is the newly infected cases, t_{avg} is the average time of the upper and lower bounds of the incubation period γ^{-1} in days as indicated in Appendix (A). Thus, the t_{avg} will be approximately five days.
The susceptible S_0 will be evaluated using the following equation:

$$S_0 = N - E_0 - I_0 - R_0 - V_0 - D_0.$$

where the states' definitions are available in Table (3.1) and the parameters' definition are defined in Table (3.2). Initially, the ranges of parameter values are assumed as follows:

$$1/7 \leqslant \gamma \leqslant 1/2, \;\; 0 \leqslant \beta \leqslant 1, \;\; 1/20 \leqslant \alpha \leqslant 1/7, \;\; and \;\; 0 \leqslant \epsilon \leqslant 1.$$

The initial guess of the parameters' values are assumed to be the average of their upper and lower bounds which were obtained based on data in Appendix(A).

The following subsection includes the curve fitting results over the whole interval assuming constant parameters.

4.3.1 The graphical results of the curve fitting over the whole interval

The following figures; Figure 4-1 , Figure 4-2, and Figure 4-3 show the curve fitting results using the investigated period as a whole (entire 60 days).

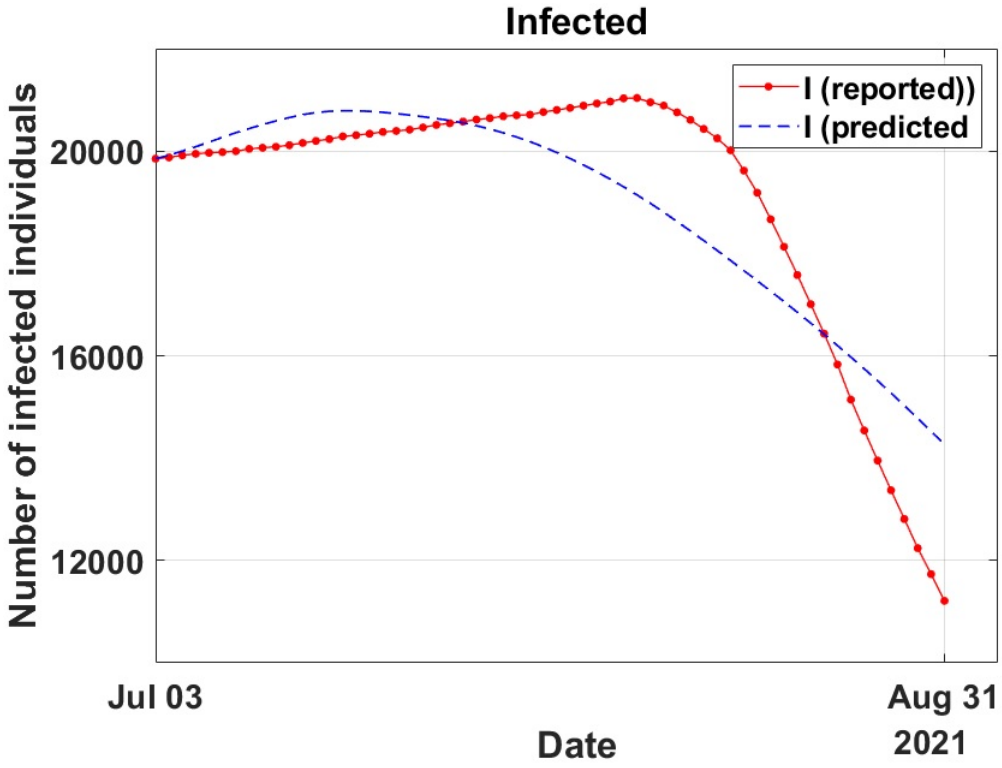

Figure 4-1: Fitted curves of reported and predicted daily numbers of infected individuals from the third of July to 31 of August 2021 (60 days) in UAE.

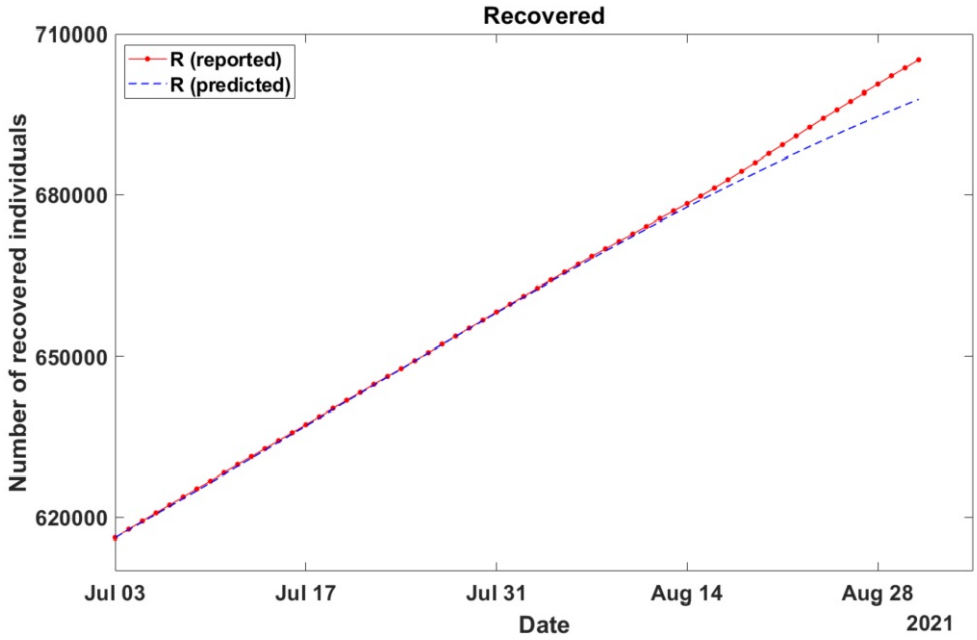

Figure 4-2: Fitted curves of reported and predicted daily numbers of recovered individuals from the third of July to 31 of August 2021 (60 days) in UAE.

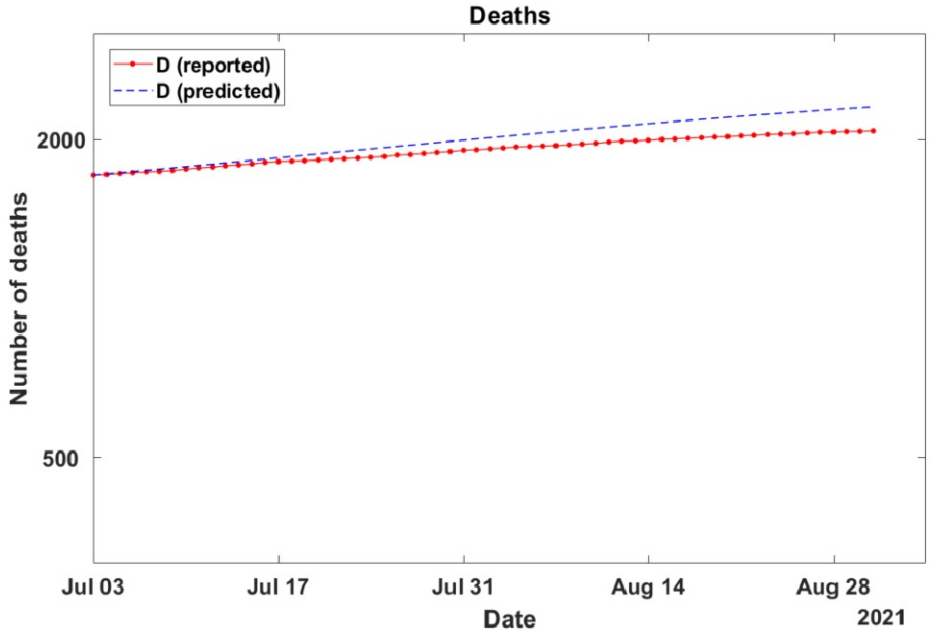

Figure 4-3: Fitted curves of reported and predicted daily numbers of deaths from the third of July to 31 of August 2021 (60 days) in UAE.

From Figure 4-1, Figure 4-2, and Figure 4-3, we conclude that assuming constant parameters is not a good choice for model prediction. In the next section, we present and use a method to estimate the model's parameters as functions of time, resulting in a hybrid switched dynamical system. The method uses the Bayesian Information Criterion (BIC) to identify the best choice for the number of switches.

4.4 General Workflow and Proposed Algorithm for the Proposed SEIR-VD Model

We employed a switched hybrid forced model as developed in [1] for dividing the main interval into sub-intervals and used the infection transmission rate β as a time-dependent forcing function while other parameters γ, α, and ϵ are constant within each sub-interval and vary from one sub-interval to another. These approaches help in capturing the variability of the parameters over the main interval.

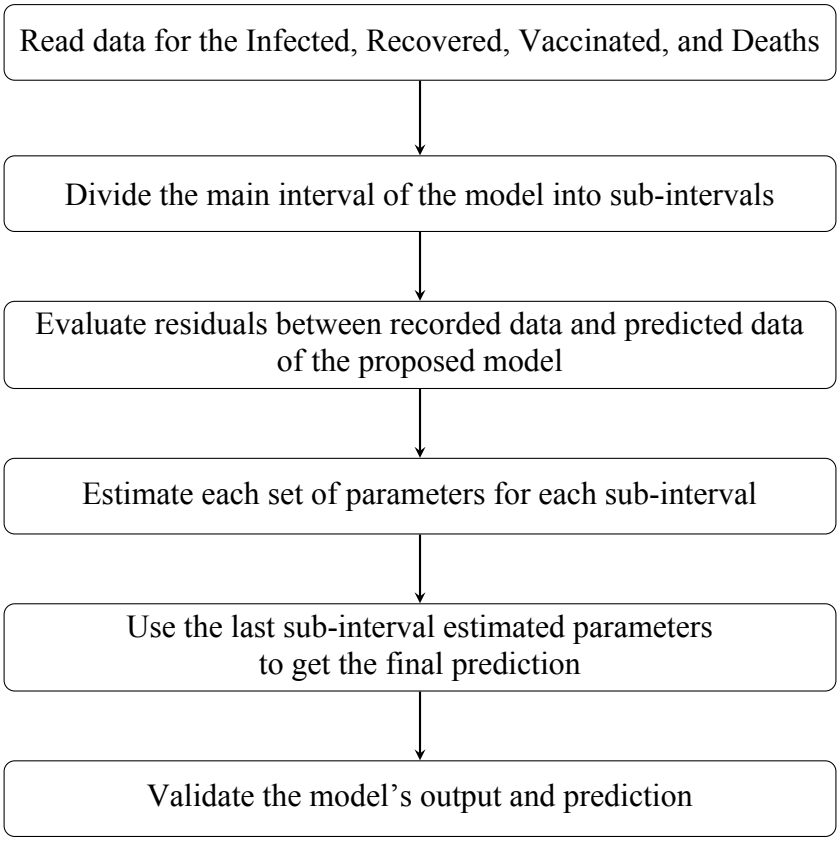

Figure 4-4: General workflow of the proposed algorithm for the SEIR-VD model

In the next subsections, we will describe in detail the implementation of the workflow in Figure (4-4) in order to construct the switched hybrid forced model.

4.5 Switched Hybrid Dynamical System Approach

A dynamical system is typically divided into two types: continuous-time dynamical systems and discrete-time dynamical systems. The combination of both types of dynamical systems is called the hybrid dynamical system [39]. Dynamical systems are widely used in different engineering applications. As examples of continuous-time dynamical systems are the classical mechanical systems and analog electronic circuits that develop in time according to physical principles such as Newton's and Kirchoff's laws. Digital systems and optimization algorithms are examples of discrete-time dynamical systems. The switched hybrid dynamical system concept entails converting hybrid time-domain solutions to a switched system. In general, a switched system is a continuous-time system that can be represented by a family of differential equations, with a switching rule or signal representing the specific differential equation that controls the state progression

at any given time point. Using a switching rule or signal will assist us in obtaining a time-varying differential equation.

Recently the switched hybrid dynamical system has been adopted in solving the epidemic ODEs models [13, 1, 37].

The switched hybrid dynamical system approach has been applied to our proposed model. It is critical to depict the COVID-19 dynamics over time to split the main interval into sub-intervals. This is due to the dramatically changing recorded data considering the external factors such as interventions and rules and regulations by policymakers.

Using the definition of the parameters ($\gamma, \beta, \alpha,$ and ϵ) as follows:
Our main interval $[t_0, T]$=60 days is split into $m = 4$ sub-intervals Δ_i. Each $\Delta_i = [t_{i-1}, t_i]$ where $i = 1, 2, 3, 4$. At t_0 we have the initial values of state variables (S, E, I, R, V, D) (4.2), and initial guess value of the parameters to be the average of their upper bound and lower bound.
Let $\omega(t) = (\gamma_i, \beta_i, \alpha_i, \epsilon_i)$ for every time i, and t $\in \Delta_i$. This means that the value of ω remains constant for each parameter component over every sub-interval while their values change from one sub-interval to another, which means that $\omega(t)$ is a piecewise constant function. Then, the switched hybrid dynamic model is represented as:

$$\begin{pmatrix} \dot{z} \\ \dot{\omega} \end{pmatrix} = \begin{pmatrix} F_\omega(t, z) \\ 0 \end{pmatrix}, \qquad z(t) = (S(t), E(t), I(t), R(t), V(t), D(t)).$$

Our six states variable (S-E-I-R-V-D) is represented as the evaluation of the z at the specific values of ω. The function $F_\omega(t, z)$ is the right hand of the system in System (3.1).

4.6 Bayesian Information Criterion (BIC) Approach

The length of each sub-interval is chosen based on the BIC approach, which has been employed for model selection among a finite set of models with different lengths. It is related to the likelihood function adjusted with a penalty term for the number of parameters that are used in the model. The penalty term is introduced to overcome the over-fitting of the model by adding more parameters. Its general formula is:

$$\text{BIC} = -2\log(\mathcal{L}(\omega \mid \text{ data })) + K\log(n). \tag{4.4}$$

Where the first term [$\log(\mathcal{L}(\omega \mid \text{ data }))$] is the maximum likelihood estimation for the given data using the set of parameters ω, K is the number of parameters to be estimated, and n is the number of observations representing the days in each sub-interval. The second term is to penalize the quality of the model towards an increment of the number of parameters used. The model with the smallest value of BIC will be selected. Under specific conditions explained and derived in [40] appropriate for the case of least-squares estimation (LSE) with errors assumed independent and identically distributed as Normal distribution, the mean squared error (MSE) is defined by:

$$MSE = \hat{\sigma}^2 = \frac{\sum_{i=1}^{n} (\hat{\epsilon}_i)^2}{n}. \tag{4.5}$$

where $\hat{\epsilon}_i$ are the estimated residuals from the fitted model.
Equation (4.4) can be written as:

$$\text{BIC} = n \log\left(\hat{\sigma}^2\right) + K \log(n). \tag{4.6}$$

The BIC Equation (4.6) has been employed in our model for selecting the best model among our proposed models with different sub-interval lengths. We implement the BIC approach to select the best model available choices of SEIR-VD models with different lengths of sub-intervals. The set Z={7, 14, 18, 20, 25, 29} includes the possible alternatives for the number of days for the sub-interval. The BIC approach is employed as follows:
Y_{pr_i} is the predicted values from the model for the infected, recovered, vaccinated, and deaths. Y_{rec_i} is the recorded data for the same states (I, R, V, and D), and $n \in Z$ is the number of days in the sub-interval for each model. Then we have $\hat{\epsilon}_i = (Y_{pr_i} - Y_{rec_i})$, and Equation (4.5) is represented as follows:

$$MSE = \hat{\sigma}^2 = \frac{\sum_{i=1}^{n} (Y_{pr_i} - Y_{rec_i})^2}{n}. \tag{4.7}$$

Use the Equation in (4.6) to select our best model sub-interval length (M) based on the minimum value of the BIC over the four states (I, R, V, and D) $\forall n \in Z$. To further optimize the minimizing of the BIC value, we choose the model of sub-interval Δ with a minimum difference between $BIC(n, Y)$ and the $\overline{BIC(Y)}$ as defined below for each

state of I, R, V, and D. This can be represented by the following formula:

$$BIC_n(Y) = BIC(n, Y) - \overline{BIC(Y)}, \quad \text{where} \quad \overline{BIC(Y)} = \min_n BIC(n, Y). \quad (4.8)$$

Hence, by using the Equation (4.8) we force the best-selected model to have a minimum value of BIC over all values of $n \in Z$ and sub-interval lengths for the infected, recovered, vaccinated, and deaths. Then, adding all 4 curves where $Y = (I, R, V, D)$ together and applying the same method:

$$M = \arg\min \sum_{Y \in (I,R,V,D)} BIC_n(Y). \quad (4.9)$$

Figure 4-5 shows the resulting $BIC_n(Y)$ total from our proposed model over the investigation period [July 3rd-August 31, 2021]. As can be seen from the figure, the optimum BIC occurs at sub-intervals with length of 14 days.

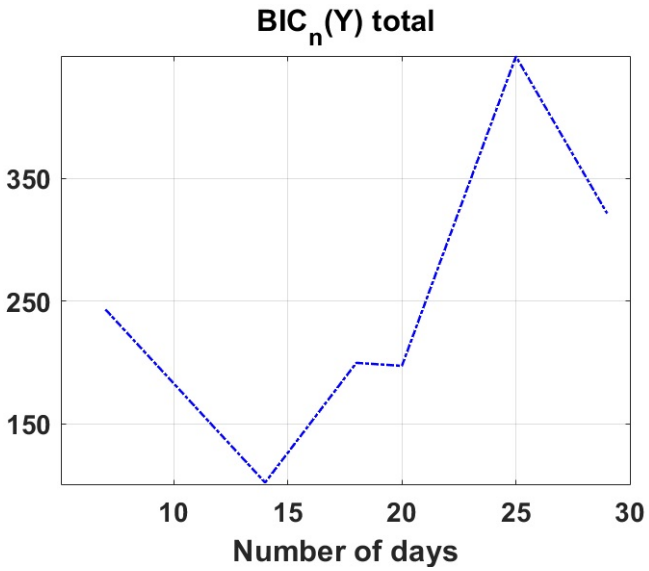

Figure 4-5: The sum value of the $BIC_n(Y)$ total for the infected, recovered, vaccinated, and deaths

After choosing the optimal length of the sub-interval, we have ensured that the last sub-interval is not short compared to its previous sub-intervals. As in our case, for 14 days over our 60 days of investigation period. Let M be the length of each sub-interval measured in days, and m be the number of sub-intervals. Our length of sub-intervals then will be 14,14,14,14,4. Therefore, we introduce the following method:
The number of sub-intervals m is calculated with respect to the total number of days

included in the investigated interval $[t_0\,, T] = [0\,, 60]$. Then each sub-interval Δ_i has a length of $M = \lfloor n/m \rfloor$ days with uniform size and $M * m = n$. If $M * m \neq n$, then the last sub-interval Δ_m will be of the length $n - (m-1) * M$ if this inequality $0 < n - m * M \leqslant \lfloor M/2 \rfloor$ holds. On the other hand, if the last inequality doesn't hold, the total number of sub-intervals will be increased by 1 $(m = m + 1)$, and the last interval will be of length $m + n - (m-1) * M$. Hence, we prevent the last sub-interval from being of a short length compared to the previous sub-intervals.

Therefore, applying the last methodology yields a total of 4 sub-intervals $\Delta_1, \Delta_2, \Delta_3, \Delta_4$, with lengths of 15,15,15,18 measured in days, respectively. Thus, we obtain the following sub-interval in dates:

$$\begin{aligned} \Delta_1 &= [03/07/2021, \quad 17/07/2021], \quad \Delta_2 = [17/07/2021, \quad 31/07/2021], \\ \Delta_3 &= [31/07/2021, \quad 14/08/2021], \quad \Delta_4 = [14/08/2021, \quad 31/08/2021]. \end{aligned} \tag{4.10}$$

Our objective function for the optimization algorithm, which is used in the parameter estimation and model calibration process, is a weighted constrained non-linear least squares function defined as follows:

$$\omega_i = \arg \min_{\omega \in BC} \sum_{j=1}^{4} \sum_{i=1}^{M} \left(Y_{pr_{(i,j)}} - Y_{rec_{(i,j)}} \right)^2 / \mu_j, \quad \mu_j = \frac{1}{M} \sum_{i=1}^{M} Y_{rec_{(i,j)}}. \tag{4.11}$$

where BC is the boundary constrains (upper bound and lowe bound) for each parameter and μ_j are positive weights used to balance the differences between data scales. The ω is the optimized vector includes the required values of all parameters $(\gamma, \beta, \alpha, \epsilon)$ during the sub-interval (Δ_i), and M is the total number of days in each sub-interval.

Solving our constrained minimization problem for parameter estimation, we get the following values over the four sub-intervals:

Table 4.1: Estimated parameter values of γ, β, α, and ϵ for the four sub-intervals.

Sub-interval	γ	β	α	ϵ
Δ_1	0.189262	0.291062	0.075734	0.000223
Δ_2	0.189037	0.330148	0.072891	0.000167
Δ_3	0.185914	0.268330	0.069307	0.000163
Δ_4	0.243514	0.169736	0.092523	0.000163
Mean	0.201932	0.264819	0.077614	0.000179

Notice that our estimation for the parameters indicates that, on average, the incubation period γ^{-1} is 5 days, and for the recovery period α^{-1} is 13 days. The fatality rate was decreasing over the main interval with a mean of 0.000179.

4.7 Infection Transmission Rate-β as a Forcing Continuous Function of Time

In order to capture the behavior of the epidemic in a sufficiently adaptable manner, we introduce the infection transmission rate $\Re_0(t)$ as a time-dependent piecewise continuous forcing function. The forced property of the $\Re_0(t)$ is imposed by employing the contact transmission rate $\beta(t)$ as a piecewise linear interpolating function as follows:

$$\beta_i(t) = \frac{t - t_i}{t_{i-1} - t_i}\beta_{i-1} + \frac{t - t_{i-1}}{t_i - t_{i-1}}\beta_i, \quad t \in \Delta_i. \tag{4.12}$$

Where time (t) is measured in days, and Δ_i is the sub-interval with $i = 1, 2, ..., m$, and $m = 4$ is the total number of sub-intervals. Notice that the following equality holds:

$$\beta_i = \beta_i(t_i) = \boldsymbol{\beta}_{i+1}(t_i), \quad i = 1, \ldots, m-1. \tag{4.13}$$

The remaining model parameters γ, α, and ϵ are assumed constant over each sub-interval (Δ_i) and evaluated using our objective function as in Equation (4.11), except at the joint point between every two consecutive intervals, where their values are assumed to be the average of the previous sub-interval estimated value and the next sub-interval estimated value in Table (4.1). Their initial guess values at t_0 are assumed to be the average of their upper and lower bounds values as given in Appendix A. This can be shown in the following equation:

$$x(t) = \begin{cases} x_1, & t = t_0, \\ x_m, & t = t_m, \\ \frac{x_i + x_{i+1}}{2}, & t = t_i, \quad 1 \leqslant i < m, \\ x_i, & t_{i-1} < t < t_i, \quad 1 \leqslant i \leqslant m. \end{cases} \tag{4.14}$$

And can be represented as the following diagram:

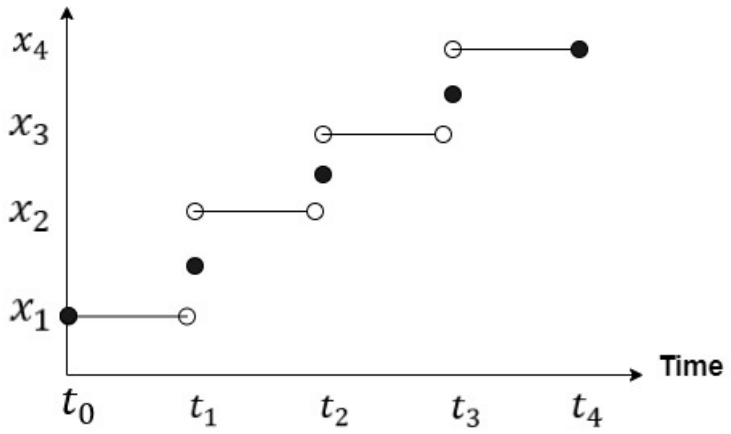

Figure 4-6: Scheme of changing parameter values over the four sub-intervals of interest

Where t indicates the time measured in days, m is the number of sub-intervals, and $x \in \{\gamma, \alpha, \epsilon\}$. The value of each parameter is not necessarily to be increasing; it can be alternating. The most important point is that within each sub-interval, a parameter must be constant.

The following graph shows the time-dependent infection transmission rate $\beta(t)$:

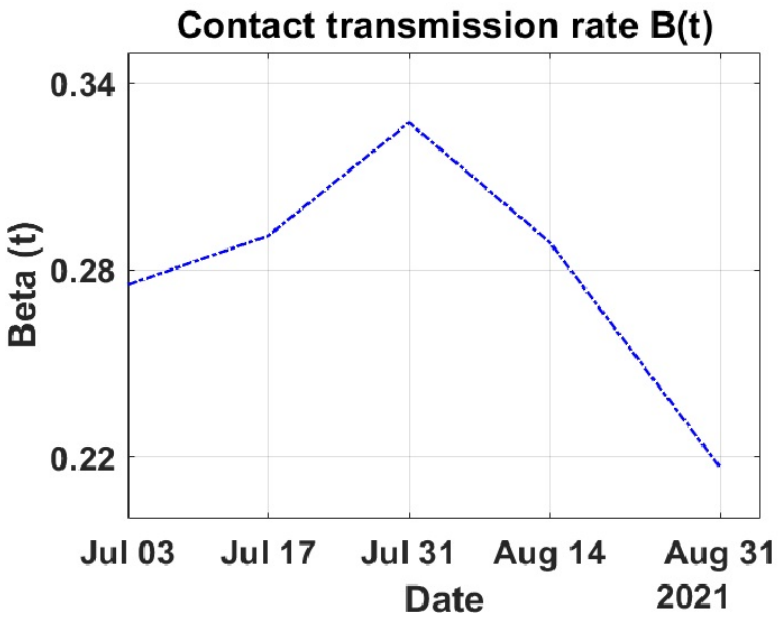

Figure 4-7: The forced continuous function $\beta(t)$.

4.7.1 Basic reproduction number as a time-dependent function

Following Equation (3.20), the basic reproduction number ($\Re_0$) without any intervention (excluding vaccine compartment) is given by:

$$\Re_0(t) = \frac{\beta(t)}{\alpha + \epsilon}. \tag{4.15}$$

Since the β is a time-dependent function, so the $\Re_0$ consequently is a time-dependent function. α and ϵ parameters are evaluated using the definition explained in the System (4.14). Figure 4-8 shows the basic reproduction number with respect to time:

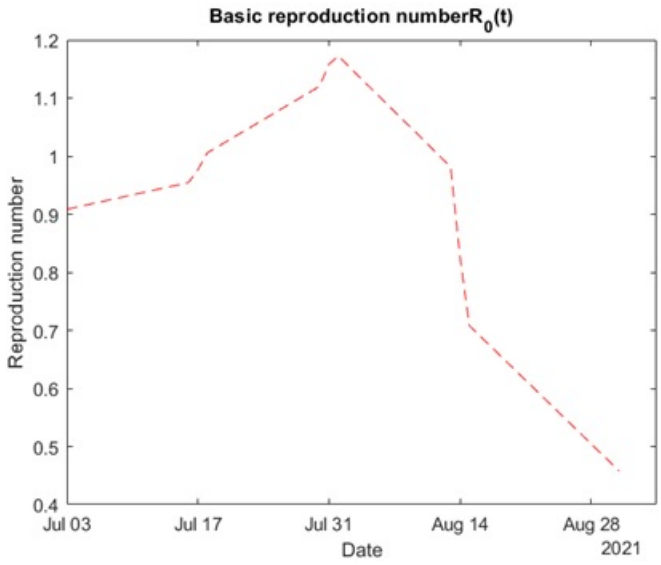

Figure 4-8: Basic reproduction number value over time.

The value of the basic reproduction number is around 1 for the first month (July). Then, its value started to decrease due to the increment of the total number of fully vaccinated individuals (around 70% of the total population) as an effective intervention against COVID-19, and also due to precautionary measures that UAE was still imposing, such as social distances and low capacities in stores and malls.

The change of $\Re_0$ due to the vaccine's inefficiency

The issue of vaccine's quality measurements and their effects on the disease spreading and individuals' immunity can be investigated through the vaccination inefficiency σ and its contribution to the basic reproduction number $\Re_0$. Where the magnitude change in $\Re_0$ can be measured due to the change in σ. Here, we can interpret those individuals who are vaccinated but, due to the vaccine inefficiency, would be able to lose their immunity and are transferred to the exposed compartment upon the β value at that moment. Hence, we could write the $\Re_0$ as follows:

$$\Re_{0\sigma}(t) = (\sigma\kappa)\Re_0(t) = (\sigma\kappa)\frac{\beta(t)}{\epsilon + \alpha}. \tag{4.16}$$

From Equation (4.16), we could evaluate the contribution of σ to the basic reproduction number and show the graphical analysis as well. The following graphs show that the vaccine's inefficiency contributes to an increment of the basic reproduction num-

ber with respect to the infection transmission rate $\beta(t)$ at the moment. Choosing $\sigma \in \{0.05, 0.1, 0.2, 0.3\}$ and simulating the model yields the following graphs of $\Re_0$ and contribution values as follows:

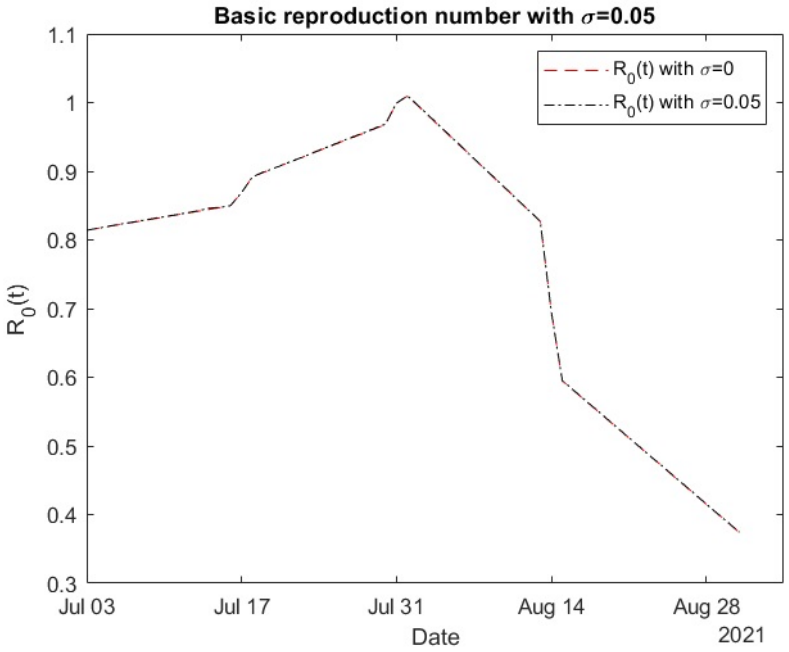

Figure 4-9: The effect of vaccine's inefficiency $\sigma = 0.05$ on $\Re_0(t)$.

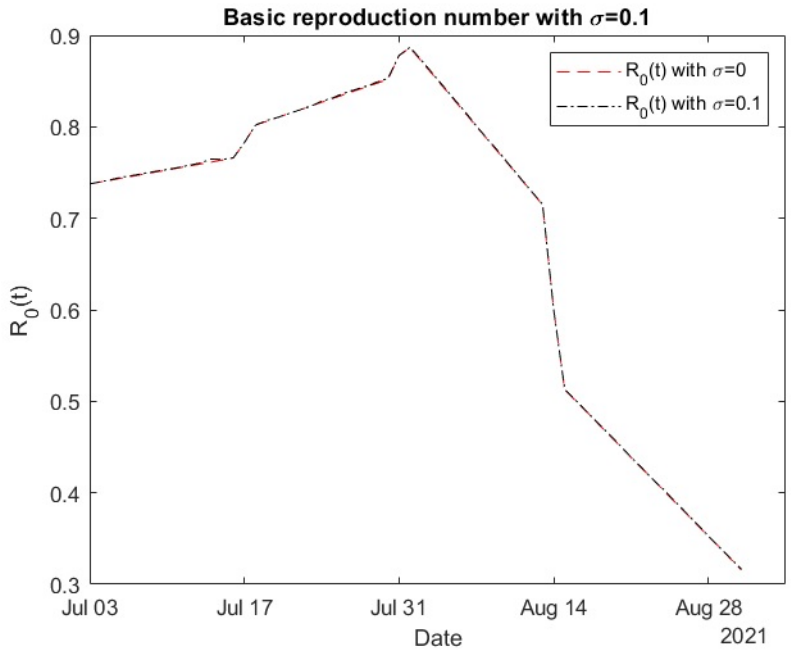

Figure 4-10: The effect of vaccine's inefficiency $\sigma = 0.1$ on $\Re_0(t)$.

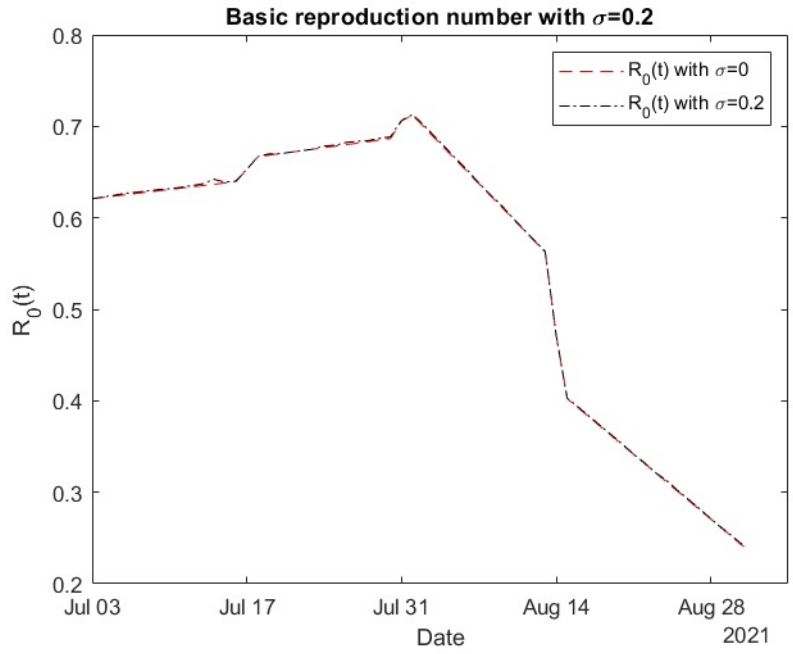

Figure 4-11: The effect of vaccine's inefficiency $\sigma = 0.2$ on $\Re_0(t)$.

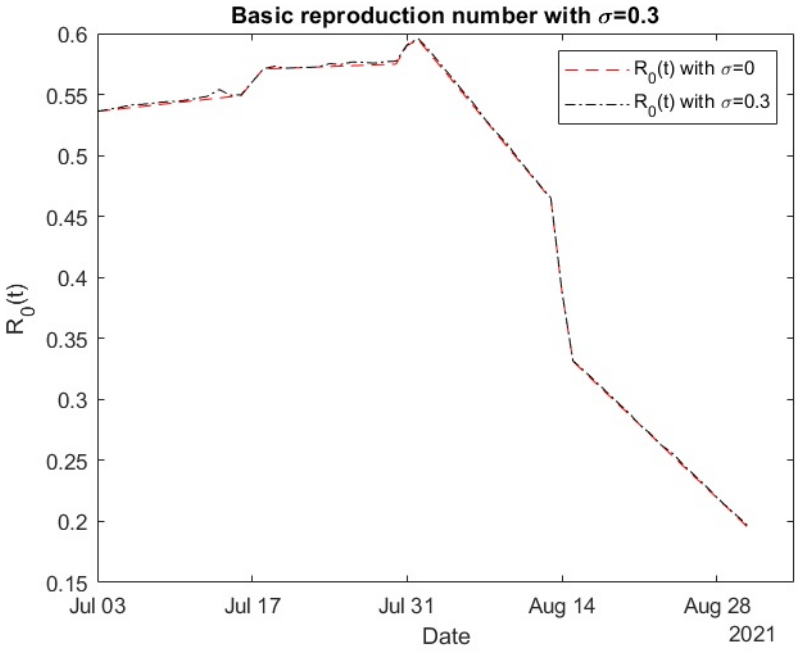

Figure 4-12: The effect of vaccine's inefficiency $\sigma = 0.3$ on $\Re_0(t)$.

Table 4.2: Vaccine's inefficiency (σ) contribution to the basic reproduction number $\Re_0(t)$.

σ	Contribution
0.05	0.00182
0.10	0.00329
0.20	0.00549
0.30	0.00708

From Table (4.2), we conclude that the values of the basic reproduction number will be increasing due to the loss of immunity from vaccinated individuals caused by vaccine inefficiency. From Table (4.2), we conclude that the increment in the σ will lead to an increment in $\Re_0$.

4.7.2 Model validation

The most crucial phase in the model construction process is model validation. The numerical results and graphs are then investigated and interpreted to verify and validate the model's output. There are two stages for the validation of curve fitting.

a) Graphical stage: where we evaluate the model by analyzing the observed data and the fitted one on the same graph, which is a critical approach for remarking the overall fluctuation of the model over time.

b) Numerical stage: where we compute statistical criteria to measure the variance between the predicted data of the model and the measured data and to confirm the goodness of the fit using the relative residual error (RRES) as follows:

$$RRES = \frac{\sum_{i=1}^{n} (Ypr_i - Yrec_i)^2}{\sum_{i=1}^{n} (Yrec_i)^2}. \tag{4.17}$$

Using the RRES in evaluating the numerical solution of the curve fitting for n days within the required sub-interval Δ_i.

In the next section, we discuss the methods and software used in solving the ODEs of the proposed model.

4.8 Results and Discussion

Under this section we show the graphs, numerical results and discuss them.

4.8.1 Original recorded data from [38]:

Before starting our parameter estimation and numerical analysis, we will show our figures for the recorded data for the infected, recovered, vaccinated and deaths as shown in the figures below for the whole period of investigation (74 days starting from 03-7-2021) the SEIR-VD model. Where we will use the first 60 days for parameter estimation and we obtained a best prediction result for the next 14 days.

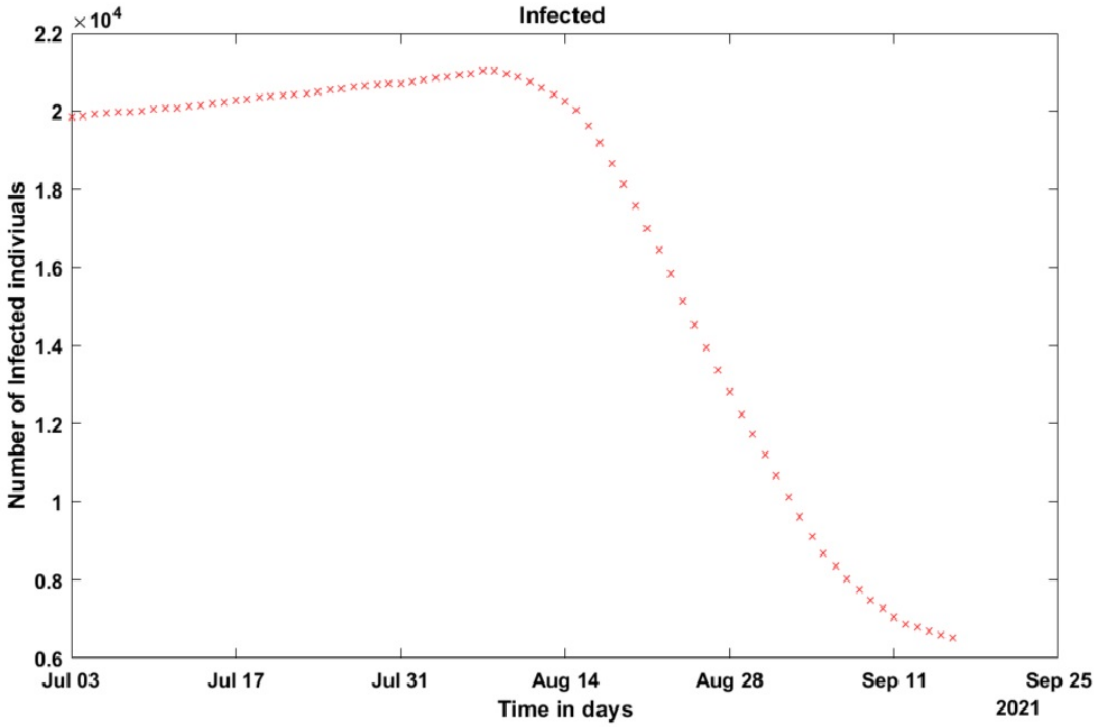

Figure 4-13: Reported daily numbers of infected individuals from the third of July to mid September 2021 in UAE as in [38].

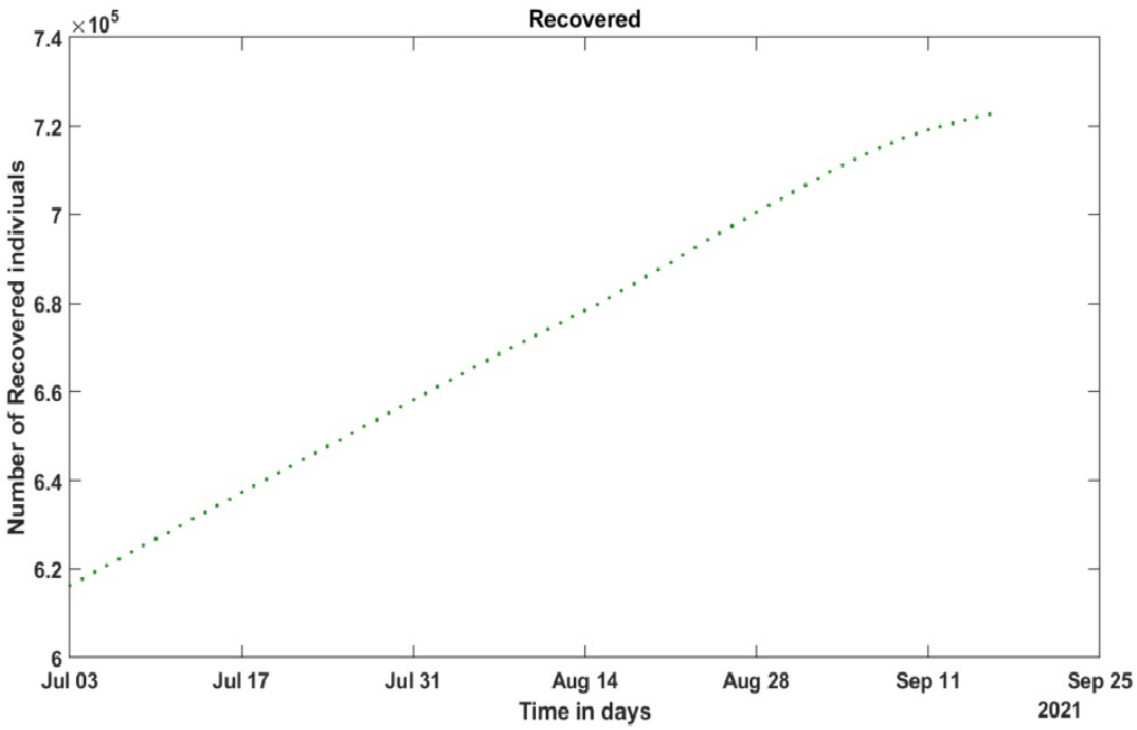

Figure 4-14: Reported daily numbers of recovered individuals from the third of July to mid September 2021 in UAE as in [38].

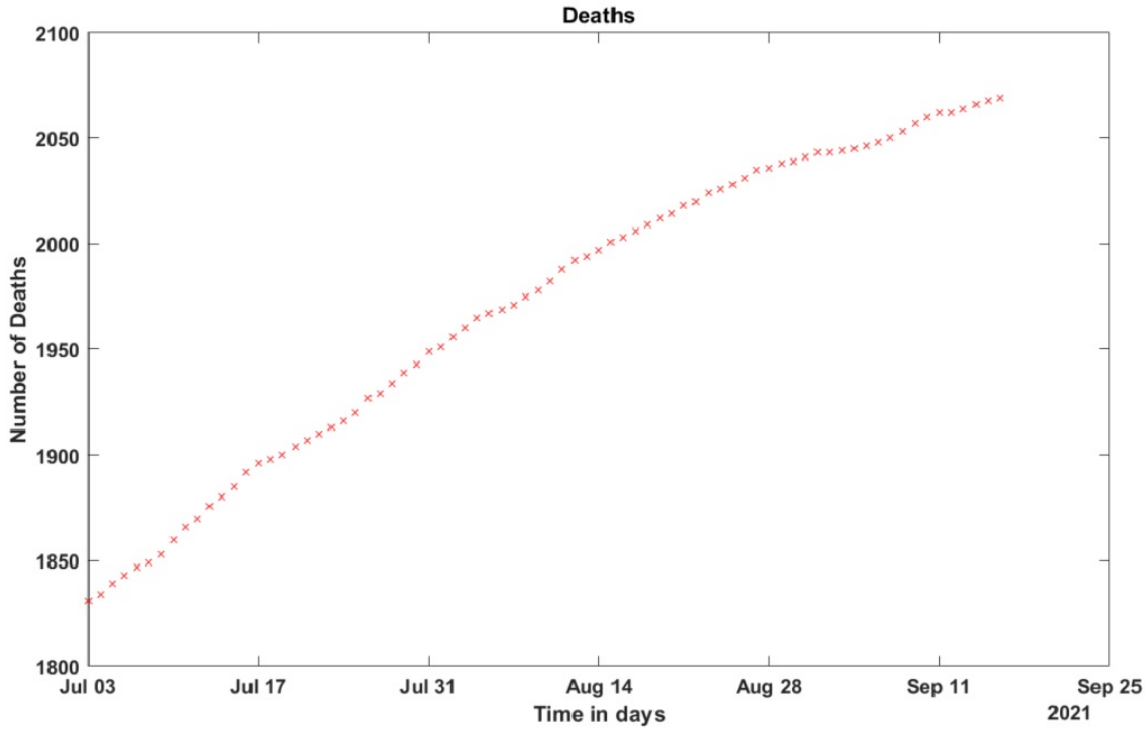

Figure 4-15: Reported daily numbers of deaths from the third of July to mid September 2021 in UAE as in [38].

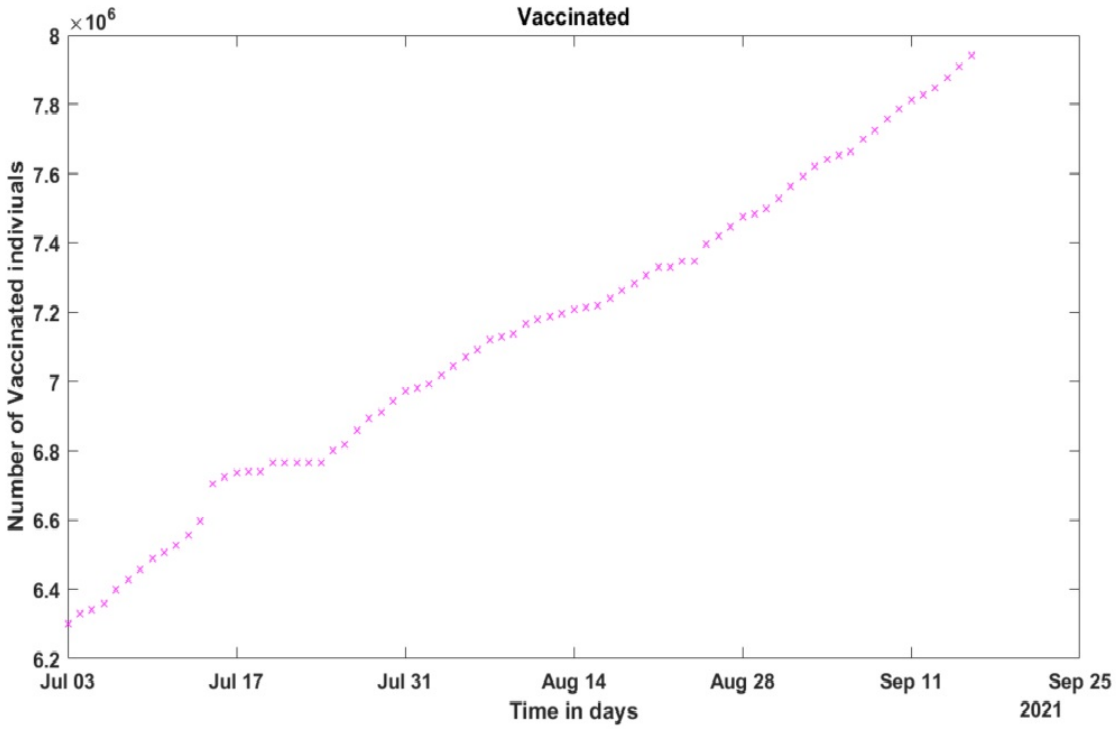

Figure 4-16: Reported daily total numbers of vaccinated individuals from the third of July to mid September 2021 in UAE as in [38].

4.8.2 The switched hybrid forced model results

While using the splitting method of the main interval into four sub-intervals ($\Delta_1, \Delta_2, \Delta_3, \Delta_4$) yields the following figures:

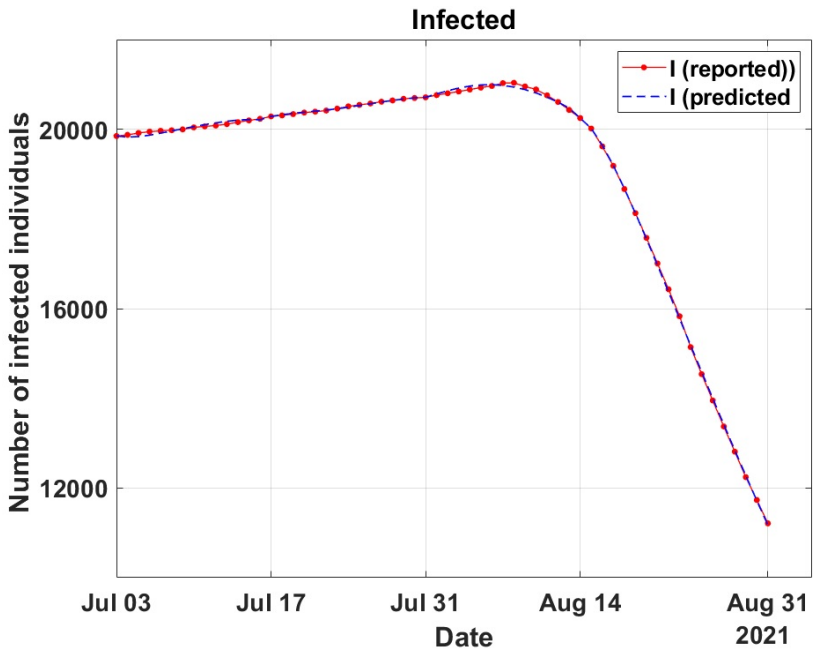

Figure 4-17: Fitted curves of infected individuals (reported and predicted from the third of July to 31 of August 2021 in UAE) [38].

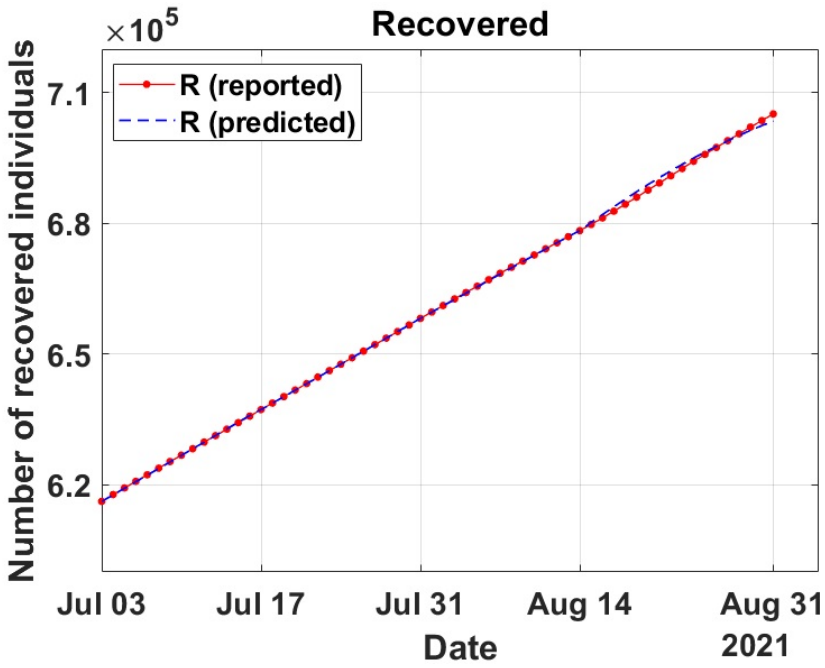

Figure 4-18: Fitted curves of recovered individuals (reported and predicted from the third of July to 31 of August 2021 in UAE) [38].

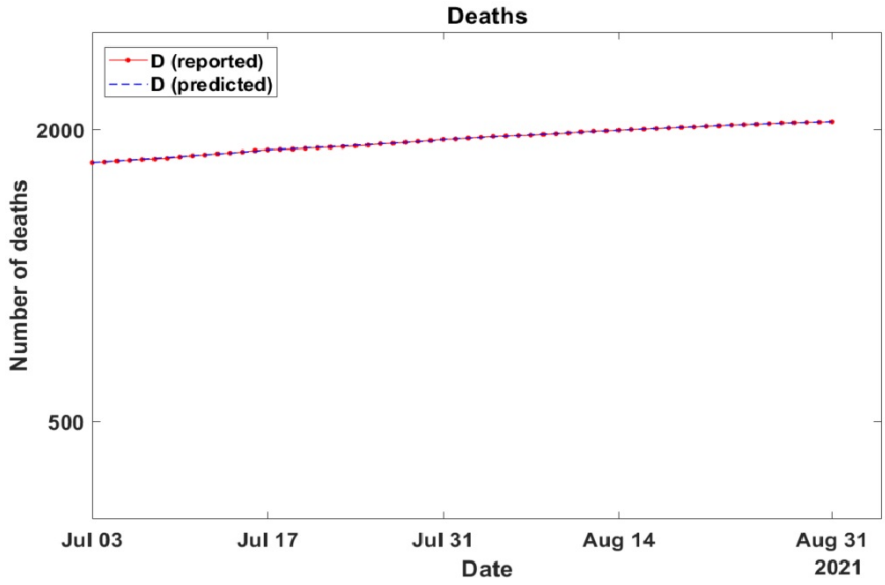

Figure 4-19: Fitted curves of deaths (reported and predicted from the third of July to 31 of August 2021 in UAE) [38].

Comparing the results of fitting the SEIR-VD model over the investigation period as a whole interval (subsection 4.3.1) and results obtained from splitting the interval into four sub-intervals with the hybrid forced model emphasizes the need of using time-dependent parameters when estimating model parameters and forecasting future trends. The relative residuals error (RRES) in Equation (4.17) are given by Table 4.3.

Table 4.3: Relative residuals of the infected (I), recovered (R), and deaths (D) for the period starting from the third of July to 31 of August 2021 in UAE.

	I	R	D
RRES	0.00213	0.001430	0.00089

4.8.3 Prediction results using the last parameters estimated in Δ_4:

For the prediction process, we used the last parameters during the last sub-interval Δ_4 as an input for the next 14 days to predict the model's output and compare these data with the reported data, the results are shown in the following figures:

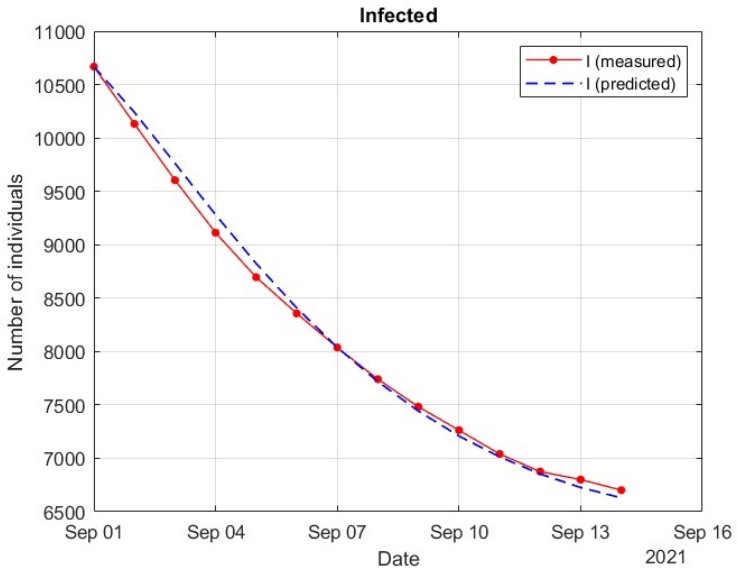

Figure 4-20: The forecasting for 14 days starting from the first of September 2021 to 14-September 2021 of infected individuals.

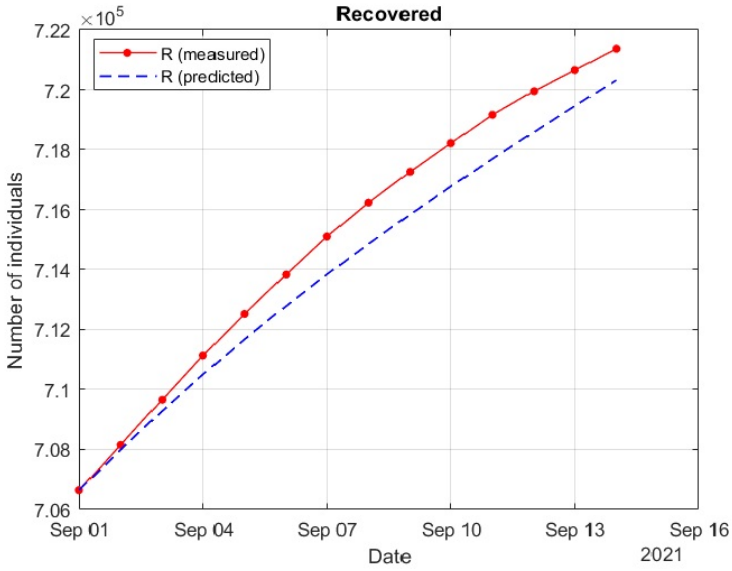

Figure 4-21: The forecasting for 14 days starting from the first of September 2021 to 14-September 2021 of recovered individuals.

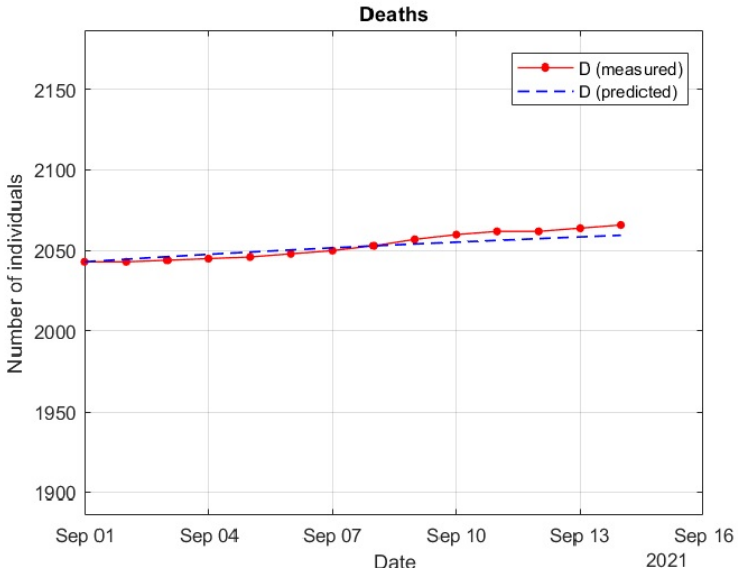

Figure 4-22: The forecasting for 14 days starting from the first of September 2021 to 14-September 2021 deaths.

The relative residuals error (RRES) in Equation (4.17) are given by Table 4.4.

Table 4.4: Relative residuals of the infected (I), recovered (R), and deaths (D) for the period starting from the first of September to mid September 2021 in UAE.

	I	R	D
RRES	0.00999	0.00145	0.00171

From the graphs in Figure (4-20,4-21, 4-22) and the relative residuals errors in Table

(4.4), we are able to recognize the quality of our prediction results.

4.8.4 Vaccination intervention and prediction:

When and how do we reach a specific percentage of fully immunized individuals of the population under various scenarios of vaccination rate increments? This inquiry will be answered via the following simulation:

From the previous last interval Δ_4 simulation process, we used the last values for the parameters $(\gamma_4, \beta_4, \alpha_4, \epsilon_4)$ in addition to introducing the vaccination rate parameter κ_4 as an input parameter to the new coming interval and letting a variable $\eta > 1$ reflecting the increment in vaccination rate κ. Hence, using the new vector for parameters during the simulation of increment of κ such as $\omega_4 = (\gamma_4, \beta_4, \sigma_4, \epsilon_4, \eta * \kappa_4)$. Assuming κ to be constant or increasing by 30% or 50% , where we have $\eta = \{1, 1.3, 1.5\}$. The following graphs are obtained after the simulation:

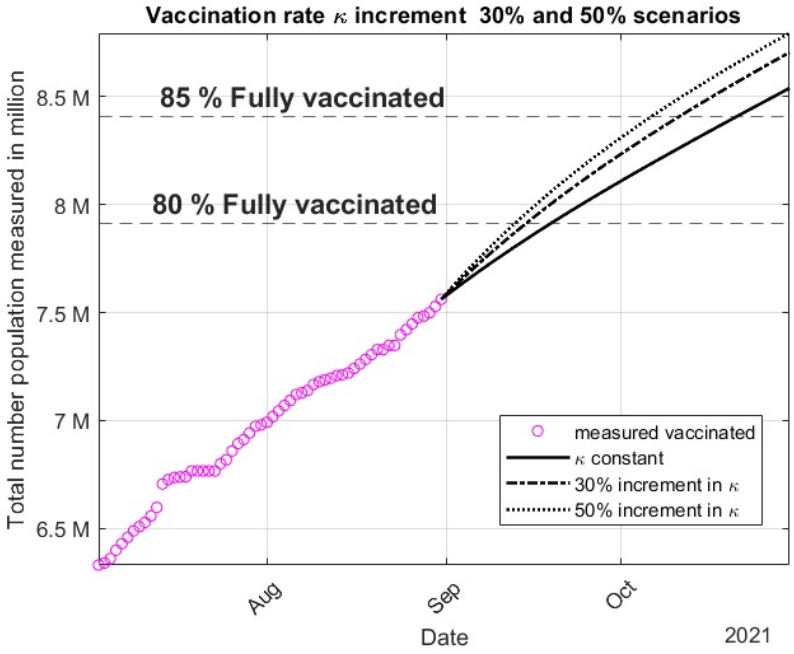

Figure 4-23: Effects of κ increment on the total number of fully vaccinated individuals.

We are able to predict when 80% and 85% of the total population will be fully vaccinated under different increments of κ scenarios (30% and 50%). This can be shown in Table (4.5) where $\kappa = 0.01285$ as calculated from the model:

Table 4.5: Required vaccinated individuals per day to reach 80% and 85%.

η	vaccinated individuals per day	80% vaccinated	85% vaccinated
1	127075	19-Sep-21	21-Oct-2021
1.3	165198	15-Sep-2021	11-Oct-2021
1.5	190613	13-Sep-2021	07-Oct-2021

Throughout different scenarios of the vaccination campaign (increment in κ), we would be able to estimate the number of individuals to be vaccinated daily to reach such a specific percentage of fully vaccinated individuals out of the total population.

Chapter 5: Conclusion, Limitations, Discussions, and Future Work

The switched hybrid forced SEIR-VD compartmental model, including six states of individuals, was proposed to investigate the COVID-19 dynamics during vaccination intervention in UAE in July 2021. All parameters are made time-dependent functions, with Beta being a continuous function while others are discrete functions. The BIC was employed for selecting the optimal interval length for splitting the main interval of investigation. Parameter estimation is achieved over a period of 60 days, starting from the third of July to the end of August 2021 (starting date of official vaccination data publication). Prediction of 14 days for the infected, recovered, and deaths was obtained under specific conditions using the estimated parameters from the last sub-interval. Graphical and numerical summaries of the prediction results were used. The effect of the vaccine's inefficiency (σ) on the basic reproduction number ($\Re_0$) was measured and investigated. We did our parameter estimation for the first two months (July and August 2021) of the vaccination intervention in UAE, where 65% of the total population is vaccinated. We managed to estimate the effect of the vaccination rate κ increment under different scenarios 30% and 50%. Thus, we could predict the time required to reach a specific percentage of immunized individuals from the total population. Moreover, we would be able to predict the required number of daily vaccinations to reach the government's goal (specific average of the total number of vaccinated individuals).

The current research study and analysis focused on the mathematical modeling and forecasting of the COVID-19 progression in UAE during the vaccination campaign. The vaccines were discovered during the last month of 2020 initially with Pfizer-BioNTech type, and the discovery continued with several types of effective vaccines during the early months of the next year of 2021 as announced by the WHO [41]. At the beginning of 2021, the UAE started the vaccination campaign, leading to around 64% of the total population in UAE getting fully vaccinated by the first of July 2021 when the FCSC started to publically report data on the daily number of vaccinations [38].

The primary limitation of the proposed model is that data always is incomplete or inaccurate, which will affect the model's output and prediction quality. The fatality rate parameter ϵ could be highly affected by underlying diseases such as age and health conditions. We believe that providing long-term prediction for any compartmental model for COVID-19 disease is imprudent and unwise, where external surrounding environ-

ment circumstances affect the disease progression dramatically. The length of immunity gained by vaccination is hard to quantify since infection data doesn't include information about vaccination history.

This study was done for the population of the UAE but can be applied to other countries and is more relevant when the switched hybrid forced approach is used for representing the mathematical model.

In general, it is worth mentioning here the famous quote of the British statistician George E. P. Box "All models are wrong, but some are useful". This aphorism refers to the trade-off between the model's complexity and ease of use, including the level of error of tolerance, rather than the general utility of models. How to make decisions in an imperfect world? In spite of this question, we must get things done and make successful decisions.

Future works can be improved by differentiating the vaccinated individuals into first and second doses, including demographic data on age and gender.

References

[1] E. Antonelli, E. L. Piccolomini, and F. Zama, "Switched forced SEIRDV compartmental models to monitor COVID-19 spread and immunization in Italy," *Infectious Disease Modelling*, vol. 7, no. 1, pp. 1–15, 2022.

[2] D. Bernoulli, "Essai d'une nouvelle analyse de la mortalité causée par la petite vérole, et des avantages de l'inoculation pour la prévenir," *Histoire de l'Acad., Roy. Sci.(Paris) avec Mem*, pp. 1–45, 1760.

[3] S. I. Oke, M. B. Matadi, and S. S. Xulu, "Optimal control analysis of a mathematical model for breast cancer," *Mathematical and Computational Applications*, vol. 23, no. 2, p. 21, 2018.

[4] T. Berge, J.-S. Lubuma, G. Moremedi, N. Morris, and R. Kondera-Shava, "A simple mathematical model for Ebola in Africa," *Journal of biological dynamics*, vol. 11, no. 1, pp. 42–74, 2017.

[5] S. Mandal, R. R. Sarkar, and S. Sinha, "Mathematical models of malaria-a review," *Malaria Journal*, vol. 10, no. 1, pp. 1–19, 2011.

[6] "World Health Organization," [Accessed:20-June-2022]. [Online]. Available: https://www.who.int/health-topics/coronavirus/coronavirus#tab=tab_1

[7] A. Adiga, D. Dubhashi, B. Lewis *et al.*, "Mathematical models for covid-19 pandemic: a comparative analysis," *Journal of the Indian Institute of Science*, vol. 100, no. 4, pp. 793–807, 2020.

[8] L. Bubniakova, "The mathematics of infectious diseases," *Comenius University Bratislava*, 2007.

[9] G. Chowell, "Fitting dynamic models to epidemic outbreaks with quantified uncertainty: A primer for parameter uncertainty, identifiability, and forecasts," *Infectious Disease Modelling*, vol. 2, no. 3, pp. 379–398, 2017.

[10] M. Garner, S. Hamilton *et al.*, "Principles of epidemiological modelling," *Revue Scientifique et Technique-OIE*, vol. 30, no. 2, p. 407, 2011.

[11] G. Perone, "An ARIMA model to forecast the spread and the final size of COVID-2019 epidemic in Italy," *MedRxiv*, 2020.

[12] L. Wang, J. Chen, and M. Marathe, "DEFSI: Deep learning based epidemic forecasting with synthetic information," *Proceedings of the AAAI Conference on Artificial Intelligence*, vol. 33, no. 01, pp. 9607–9612, 2019.

[13] M. Ala'raj, M. Majdalawieh, and N. Nizamuddin, "Modeling and forecasting of COVID-19 using a hybrid dynamic model based on SEIRD with ARIMA corrections," *Infectious Disease Modelling*, vol. 6, pp. 98–111, 2021.

[14] N. ben Khedher, L. Kolsi, and H. Alsaif, "A multi-stage SEIR model to predict the potential of a new COVID-19 wave in KSA after lifting all travel restrictions," *Alexandria Engineering Journal*, vol. 60, no. 4, pp. 3965–3974, 2021.

[15] R. Ghostine, M. Gharamti, S. Hassrouny, and I. Hoteit, "An extended SEIR model with vaccination for forecasting the COVID-19 pandemic in Saudi Arabia using an Ensemble Kalman Filter," *Mathematics*, vol. 9, no. 6, p. 636, 2021.

[16] W. O. Kermack and A. G. McKendrick, "A contribution to the mathematical theory of epidemics," *Proceedings of the royal society of london. Series A, Containing papers of a mathematical and physical character*, vol. 115, no. 772, pp. 700–721, 1927.

[17] P. E. Lekone and B. F. Finkenstädt, "Statistical inference in a stochastic epidemic SEIR model with control intervention: Ebola as a case study," *Biometrics*, vol. 62, no. 4, pp. 1170–1177, 2006.

[18] G. Pandey, P. Chaudhary, R. Gupta, and S. Pal, "SEIR and regression model based COVID-19 outbreak predictions in India," *arXiv preprint arXiv:2004.00958*, 2020.

[19] S. Annas, M. I. Pratama, M. Rifandi, W. Sanusi, and S. Side, "Stability analysis and numerical simulation of SEIR model for pandemic COVID-19 spread in Indonesia," *Chaos, Solitons & Fractals*, vol. 139, p. 110072, 2020.

[20] G. S. Tuteja, "Stability and Numerical Investigation of modified SEIR model with Vaccination and Life-long Immunity," *Eur. J. Mol. Clin. Med*, vol. 7, pp. 3034–3044, 2020.

[21] M. J. Keeling and P. Rohani, "Modeling infectious diseases in humans and animals," in *Modeling Infectious Diseases in Humans and Animals*. Princeton University Press, 2011.

[22] J. Tolles and T. Luong, "Modeling epidemics with compartmental models," *Jama*, vol. 323, no. 24, pp. 2515–2516, 2020.

[23] Q. Liu, Z. Liu, J. Zhu, Y. Zhu, D. Li, Z. Gao, L. Zhou, Y. Tang, X. Zhang, J. Yang *et al.*, "Assessing the global tendency of COVID-19 outbreak," *MedRxiv*, 2020.

[24] "UAE: Recovered Covid patients may have immunity for 9 months," [Accessed:20-June-2022], [Online]. Available: https://www.khaleej-times.com/coronavirus-pandemic/uae-recovered-covid-patients-may-have-immunity-for-9-months.

[25] P. L. Delamater, E. J. Street, T. F. Leslie, Y. T. Yang, and K. H. Jacobsen, "Complexity of the basic reproduction number," *Emerging Infectious Diseases*, vol. 25, no. 1, p. 1, 2019.

[26] R. M. Anderson and R. M. May, *Infectious Diseases of Humans: Dynamics and Control*. Oxford University Press, 1992.

[27] P. Van den Driessche and J. Watmough, "Further notes on the basic reproduction number," *Mathematical Epidemiology*, vol. 1945, pp. 159–178, 2008.

[28] E. X. DeJesus and C. Kaufman, "Routh-Hurwitz criterion in the examination of eigenvalues of a system of nonlinear ordinary differential equations," *Physical Review A*, vol. 35, no. 12, p. 5288, 1987.

[29] O. Diekmann, J. A. P. Heesterbeek, and J. A. Metz, "On the definition and the computation of the basic reproduction ratio R0 in models for infectious diseases in heterogeneous populations," *Journal of Mathematical Biology*, vol. 28, no. 4, pp. 365–382, 1990.

[30] P. Van den Driessche and J. Watmough, "Reproduction numbers and sub-threshold endemic equilibria for compartmental models of disease transmission," *Mathematical Biosciences*, vol. 180, no. 1-2, pp. 29–48, 2002.

[31] C. Mitchell and C. Kribs, "A comparison of methods for calculating the basic reproductive number for periodic epidemic systems," *Bulletin of Mathematical Biology*, vol. 79, no. 8, pp. 1846–1869, 2017.

[32] T. Britton and D. Ouédraogo, "SEIRS epidemics with disease fatalities in growing populations," *Mathematical Biosciences*, vol. 296, pp. 45–59, 2018.

[33] M. Martcheva, *An Introduction to Mathematical Epidemiology*. Springer, 2015, vol. 61.

[34] G. Chowell, N. W. Hengartner, C. Castillo-Chavez, P. W. Fenimore, and J. M. Hyman, "The basic reproductive number of Ebola and the effects of public health measures: the cases of Congo and Uganda," *Journal of Theoretical Biology*, vol. 229, no. 1, pp. 119–126, 2004.

[35] L. López and X. Rodo, "A modified SEIR model to predict the COVID-19 outbreak in Spain and Italy: simulating control scenarios and multi-scale epidemics," *Results in Physics*, vol. 21, p. 103746, 2021.

[36] O. Kounchev, G. Simeonov, and Z. Kuncheva, "The TVBG-SEIR spline model for analysis of COVID-19 spread, and a Tool for prediction scenarios," *arXiv preprint arXiv:2004.11338*, 2020.

[37] E. Loli Piccolomini and F. Zama, "Monitoring Italian COVID-19 spread by a forced SEIRD model," *PloS one*, vol. 15, no. 8, p. e0237417, 2020.

[38] "Federal Competitiveness and Statstics Centre," [Accessed:20-June-2022]. [Online]. Available: https://fcsc.gov.ae/en-us/Pages/Covid19/UAE-Covid-19-Updates.aspx

[39] R. Goebel, R. G. Sanfelice, and A. R. Teel, "Hybrid dynamical systems," in *Hybrid Dynamical Systems*. Princeton University Press, 2012.

[40] K. P. Burnham and D. R. Anderson, "Multimodel inference: Understanding AIC and BIC in model selection," *Sociological Methods & Research*, vol. 33, no. 2, pp. 261–304, 2004.

[41] "COVID-19 Vaccines," [Accessed:20-June-2022]. [Online]. Available: https://www.who.int/emergencies/diseases/novel-coronavirus-2019/covid-19-vaccines

[42] "United Arab Emirates: Data and statistics," [Accessed:20-June-2022]. [Online]. Available: https://knoema.com/atlas/United-Arab-Emirates

[43] "UAE Death Rate 1950-2022," [Accessed:20-June-2022]. [Online]. Available: https://www.macrotrends.net/countries/ARE/uae/death-rate

[44] "Coronavirus Incubation Period," [Accessed:20-June-2022]. [Online]. Available: https://www.worldometers.info/coronavirus/coronavirus-incubation-period/

[45] F. Zhou, T. Yu, R. Du, G. Fan, Y. Liu, Z. Liu, J. Xiang, Y. Wang, B. Song, X. Gu *et al.*, "Clinical course and risk factors for mortality of adult inpatients with COVID-19 in Wuhan, China: a retrospective cohort study," *The Lancet*, vol. 395, no. 10229, pp. 1054–1062, 2020.

[46] "COVID-19 Vaccine Efficacy Summary," [Accessed:20-June-2022]. [Online]. Available: http://www.healthdata.org/covid/covid-19-vaccine-efficacy-summary

Appendix A

List of parameters and their values.

Parameter	Name	Values (ranges) lower bound & upper bound	Reference
N	total population	9,890,400	[42]
μ	Natural death rate	$4.71 * 10^{-7}$	[43]
β	Transmission rate (S state to E state)	$0 \leqslant \beta \leqslant 1$	estimated from calibration
γ	Transmission rate (E state to I state)	$0.1429 \leqslant \gamma \leqslant 0.5$	[23], [44]
α	Recovery rate (I state to R state)	$0.05 \leqslant \alpha \leqslant 0.1429$	[45]
δ	Immunity loss	$0.0037 \leqslant \delta \leqslant 0.0056$	[24]
ϵ	Fatality rate due to covid19	$0 \leqslant \epsilon \leqslant 1$	estimated from calibration
σ	vaccination inefficiency $0 \leqslant \sigma \leqslant 1$	$0.05 \leqslant \sigma \leqslant 0.3$	[46]
κ	Vaccination rate out of Susceptible state)	$0 \leqslant \kappa \leqslant 1$	calculated

Appendix B

Recorded data starting from 3^{rd} of July 2021

Day	Newly infected	Infected	Recovered	Deaths	Vaccinated
1	1632	19,849	616,197	1,831	6300185
2	1599	19,875	617,767	1,834	6329856
3	1573	19,916	619,294	1,839	6339746
4	1552	19,946	620,812	1,843	6359527
5	1513	19,966	622,301	1,847	6399089
6	1539	19,978	623,826	1,849	6428760
7	1529	19,997	625,332	1,853	6458431
8	1520	20,042	626,800	1,860	6488102
9	1518	20,064	628,290	1,866	6507883
10	1542	20,083	629,809	1,870	6527664
11	1522	20,114	631,294	1,876	6557335
12	1529	20,158	632,775	1,880	6596897
13	1541	20,197	634,272	1,885	6705691
14	1530	20,233	635,759	1,892	6725472
15	1565	20,286	637,267	1,896	6735362
16	1529	20,309	638,771	1,898	6738330
17	1508	20,338	640,248	1,900	6739319
18	1541	20,373	641,750	1,904	6766023
19	1506	20,392	643,234	1,907	6766023
20	1547	20,417	644,753	1,910	6766023
21	1521	20,461	646,227	1,913	6766023
22	1507	20,510	647,682	1,916	6766023
23	1528	20,543	649,173	1,920	6799650
24	1549	20,575	650,683	1,927	6817453
25	1539	20,615	652,180	1,929	6858992

Continued on next page

- - continued from previous page

Day	Infected (new)	Infected (active)	Recovered	Deaths	Vaccinated
26	1527	20,642	653,675	1,934	6892620
27	1550	20,679	655,183	1,939	6911412
28	1520	20,698	656,680	1,943	6942072
29	1537	20,711	658,198	1,949	6972732
30	1519	20,762	659,664	1,951	6979655
31	1537	20,802	661,156	1,956	6991524
32	1548	20,842	662,660	1,960	7018228
33	1519	20,886	664,130	1,965	7043943
34	1508	20,929	665,593	1,967	7069658
35	1520	20,966	667,074	1,969	7092406
36	1545	21,029	668,554	1,971	7120099
37	1410	21,036	669,953	1,975	7128011
38	1321	20,954	671,353	1,978	7138891
39	1334	20,888	672,749	1,982	7166584
40	1287	20,756	674,162	1,988	7179441
41	1260	20,608	675,566	1,992	7188343
42	1215	20,431	676,956	1,994	7196255
43	1206	20,249	678,341	1,997	7207135
44	1189	20,015	679,760	2,001	7212080
45	1109	19,617	681,265	2,003	7219992
46	1115	19,185	682,809	2,006	7240762
47	1089	18,666	684,414	2,009	7261532
48	1077	18,129	686,025	2,012	7283291
49	1070	17,578	687,644	2,014	7305049
50	1066	17,007	689,277	2,018	7328786
51	1076	16,432	690,926	2,020	7328786
52	1060	15,829	692,585	2,024	7347578
53	990	15,142	694,260	2,026	7347578

Continued on next page

- - continued from previous page

Day	Infected (new)	Infected (active)	Recovered	Deaths	Vaccinated
54	983	14,540	695,843	2,028	7397030
55	991	13,952	697,419	2,031	7420767
56	994	13,372	698,989	2,035	7447471
57	998	12,810	700,548	2,036	7476153
58	987	12,241	702,102	2,038	7484066
59	993	11,732	703,603	2,039	7498901
60	996	11,211	705,118	2,041	7528573
61	985	10,668	706,644	2,043	7561211
62	975	10,132	708,155	2,043	7592860
63	978	9,605	709,659	2,044	7620553
64	984	9,113	711,134	2,045	7642312
65	971	8,696	712,521	2,046	7651213
66	977	8,357	713,835	2,048	7665060
67	952	8,038	715,104	2,050	7699676
68	833	7,741	716,231	2,053	7726381
69	772	7,483	717,257	2,057	7758030
70	744	7,263	718,218	2,060	7785723
71	725	7,041	719,163	2,062	7811438
72	620	6,876	719,948	2,062	7827263
73	632	6,801	720,653	2,064	7846054
74	617	6,702	721,367	2,066	7875726
75	608	6,602	722,073	2,068	7908364
76	564	6,515	722,723	2,069	7941002
77	521	6,420	723,337	2,071	7973641
78	471	6,285	723,941	2,073	8010235
79	391	6,169	724,446	2,075	8019136
80	313	6,071	724,855	2,077	8034961

Vita

Manal W. Almuzini was born in 1972, in Kuwait. She obtained her Bachelor of Science degree in Computer Engineerig in 1996, from Applied Science University-Jordan. Moreover, she obtained an Excutive Master of Business Administration in 2006 from SZABIST-Dubai campus. Currently, she is working as a registration supervisor at Ajman University, UAE.